Journal of Medicinal Chemistry

Article

Leveraging a Low Affinity Diazaspiro Orthosteric Fragment to Reduce Dopamine D3 Receptor (D3R) Ligand Promiscuity Across Highly Conserved Aminergic G-Protein-Coupled Receptors (GPCRs)

Sean W. Reilly, Aladdin A. Riad, Chia-Ju Hsieh, Kristoffer Sahlholm, Daniel A. Jacome, Suzy Griffin, Michelle Taylor, Chi-Chang Weng, Kuiying Xu, Nathan Kirschner, Robert R. Luedtke, Christopher Parry, Shipra Malhotra, John Karanicolas, and Robert H. Mach

J. Med. Chem., **Just Accepted Manuscript** • DOI: 10.1021/acs.jmedchem.9b00412 • Publication Date (Web): 25 Apr 2019

Just Accepted

ACS Publications

is published by the American Chemical Society. 1155 Sixteenth Street N.W., Washington, DC 20036

Leveraging a Low Affinity Diazaspiro Orthosteric Fragment to Reduce Dopamine D_3 Receptor (D_3R) Ligand Promiscuity Across Highly Conserved Aminergic G-Protein-Coupled Receptors (GPCRs)

Sean W. Reilly,[†] Aladdin A. Riad,[†] Chia-Ju Hsieh,[†] Kristoffer Sahlholm,[†] Daniel A. Jacome,[‡] Suzy Griffin,[§] Michelle Taylor,[§] Chi-Chang Weng,[†] Kuiying Xu,[†] Nathan Kirschner,[†] Robert R. Luedtke,[§] Christopher Parry,[⊤] Shipra Malhotra,[⊤] John Karanicolas,[⊤] and Robert H. Mach[*,†]

[†]Department of Radiology, Perelman School of Medicine, University of Pennsylvania, Philadelphia, Pennsylvania 19104, United States

[‡]Department of Systems Pharmacology and Translational Therapeutics, University of Pennsylvania, 421 Curie Boulevard, Philadelphia, Pennsylvania 19104, United States

[§]Department of Pharmacology and Neuroscience, University of North Texas Health Science Center, 3500 Camp Bowie Boulevard, Fort Worth, Texas 76107, United States

[⊤]Program in Molecular Therapeutics, Fox Chase Cancer Center, 333 Cottman Avenue, Philadelphia, Pennsylvania 19111, United States

ABSTRACT: Previously we reported a 3-(2-methoxyphenyl)-9-(3-((4-methyl-5-phenyl-4H-1,2,4-triazol-3-yl)thio)propyl)-3,9-diazaspiro[5.5]undecane (**1**) compound with excellent dopamine D_3 receptor (D_3R) affinity (D_3R K_i = 12.0 nM) and selectivity (D_2R/D_3R ratio = 905). Herein, we present derivatives of **1** with comparable D_3R affinity (**32**, D_3R K_i = 3.2 nM, D_2R/D_3R ratio = 60), and selectivity (**30**, D_3R K_i = 21.0 nM, D_2R/D_3R ratio = 934). Fragmentation of **1** revealed orthosteric fragment **5a** to express an unusually low D_3R affinity (K_i = 2.7 μM). Compared to piperazine congener **31**, which retains a high affinity orthosteric fragment (**5d**, D_3R K_i = 23.9 nM), **1** was found to be more selective for the D_3R among D_1- and D_2-like receptors, and exhibited negligible off-target interactions at serotoninergic and adrenergic GPCRs, common off-target sites for piperazine-containing D_3R scaffolds. This study provides a unique rationale for implementing weakly potent orthosteric fragments into D_3R ligand systems to minimize drug promiscuity at other aminergic GPCR sites.

INTRODUCTION

The dopamine D_3 receptor (D_3R) is a G protein-coupled receptor (GPCR), viewed as a pharmacotherapeutic target for numerous neurological and psychiatric disorders as well as drug addiction.[1, 2] Targeting this D_2-like receptor is a strategy for schizophrenia drug development due to the unwanted extrapyramidal side-effects elicited with many typical antipsychotics.[3] The appeal of D_3R for drug addiction therapeutics stems from the high expression of this protein in the mesolimbic pathway, a region of the brain implicated in reward and motivation.[4] Human postmortem studies showing enhanced expression of the D_3R in drug exposed brains has further validated the clinical importance of this receptor for substance abuse disorders (SUD).[5] Selective engagement of this receptor is also of considerable interest for positron-emission tomography (PET) imaging applications to further our understanding and elucidate the complex molecular mechanisms of drug addiction.[6-9]

Development of high affinity D_3R selective ligands begins with a fragment-based approach in which the binding profiles of amino core synthons are examined at the orthosteric binding site (OBS) of the receptor. This region contains a highly conserved Asp110 [3.32] residue which forms a salt-bridge interaction with the protonated nitrogen of the amino core in the ligand scaffold affording receptor recognintion.[10] Due to the high degree of homology between the D_3R and the D_2R in this domain, the ligand must then extend into a secondary binding pocket (SBP) containing residues unique to each receptor in order to confer D_3R selectivity.[10-12] However, the Asp110 [3.32] that forms the critical receptor-ligand interaction is also greatly conserved across other aminergic GPCRs.[13] Thus, synthesizing D_3R selective compounds, that concomitantly engage the Asp110 [3.32] residue and exhibit minimal off-target interactions continues to be problematic. As such, there have been no clinically viable D_3R selective therapeutic or PET imaging agent reported to date, preventing us from exploring the therapeutic potential of this receptor.

Recently, we reported a new class of D_3R selective compounds containing spirodiamine systems as an alternative to the piperazine amino core (**Figure 1**).[14] In this study, we synthesized and evaluated analogues and fragments of **1** in order to identify the structural determinants responsible for ligand affinity and selectivity at the D_3R. Compared to the excellent binding profile of aryl piperazine orthosteric fragment **5d** (K_i = 23.9 nM) of ligand **31**, we found sython **5a** of **1** to be bind with lower affinity (K_i > 2 μM). Computational ligand docking studies were performed in order to elucidate the binding mode of **1**, and other select compounds, within the D_3R crystal structure (3PBL). Finally, the pharmacological behavior of **1** and **31** was screened across all D_1 (D_1R and D_5R)- and D_2 (D_2R, D_3R and D_4R)-like receptors, and select aminergic GPCRs, revealing **1** to be a more selective ligand for the D_3R with less off-target interactions. These results provide rationale for utilizing primary pharmacophores with limited affinity for the highly conserved orthosteric binding pocket (OBP) of the receptor in order to develop selective D_3R ligands with minimized off-target interactions.

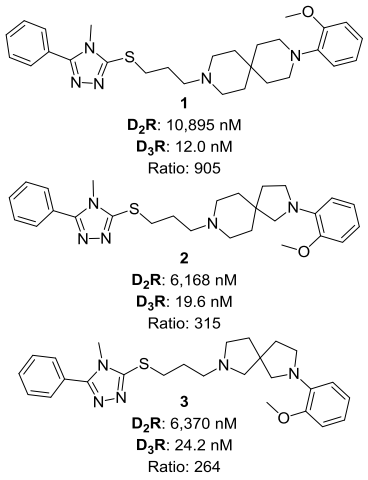

Figure 1. Lead compounds identified with diazaspiro amino systems.

RESULTS AND DISCUSSION

Chemistry. Synthesis of arylated diazaspiro and piperazine systems was achieved in excellent yields following our previously reported Pd C–N cross-coupling reports outlined in Scheme 1.[15, 16] Unsaturated diazaspiro[5.5]undec-1-ene motif **4a,** a presumed cross-coupling *β*-hydride elimination side-product, was able to be obtained, albeit in low yields (<10%). Following removal of the BOC protecting groups from **4b**, **4c**, and **4e** with trifluoroacetic acid (TFA) and basification, the corresponding free-amine intermediates **4b'**, **4c'**, and **4e'** were *N*-alkylated with 1-bromobutane at room temperature in acetone to afford desired synthons **5a-c**. Similarly, *S*-alkylation of commercially available 4-methyl-5-phenyl-4H-1,2,4-triazole-3-thiol with the appropriate alkylating reagent yielded **6a-b** in good yields. Formation of 1,2,4-triazole fragments **6c-e**, and **6g** were readily accessed by reacting **6b** with the desired amine in the presence of Cs_2CO_3 under refluxing conditions. BOC-deprotection with TFA, followed by base neutralization, afforded the final free-amine fragments **6f** and **6h**.

Scheme 1. Synthesis of Fragmented Synthons[a]

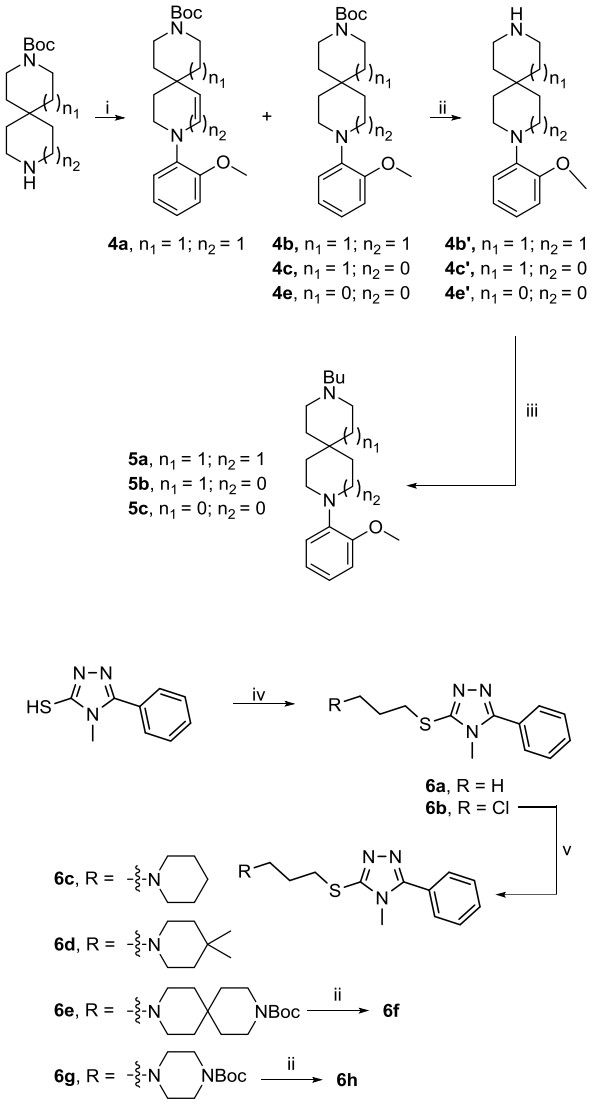

[a]Reagents and conditions: (i) $Pd_2(dba)_3$, RuPhos, aryl halide, diazaspiro reagent, NaO*t*-Bu, dioxane, 100 °C, 20 min; (ii) TFA, CH_2Cl_2, rt, 3 h; (iii) 1-bromobutane, K_2CO_3, acetone, rt, 12 h; (iv) alkylating reagent, K_2CO_3, acetone, rt, 12 h; (v) amine, Cs_2CO_3, ACN, 70 °C, 8h.

Scheme 2 briefly illustrates the general synthesis, disclosed in our previous report[14], used to obtain ligands **1**-**3**, and **7**-**34**. Aryl amide scaffolds **35**-**37** were prepared by reacting **4b'** with 2-(4-bromobutyl)isoindoline-1,3-dione, to afford precursor **E** in a modest yield of 64%. Next, **E** was treated with hydrazine in refluxing EtOH to afford free-amine intermediate **F** in excellent yield (97%). Finally,

benzamide compounds **35-36** were synthesized by coupling **F** with the respective benzoic acid in the presence of 1-hydroxybenzotriazole (HOBt) hydrate and 1-ethyl-3-(3'-dimethylaminopropyl)carbodiimide (EDC) in dichloromethane at room temperature. Following our 2011 report[17], synthon **4b'** was *N*-alkylated with intermediate **G**, to afford the aripiprazole analogue **37** in modest yield (62%).

Scheme 2. General Synthesis of Compounds 1-3 and 7-37[a]

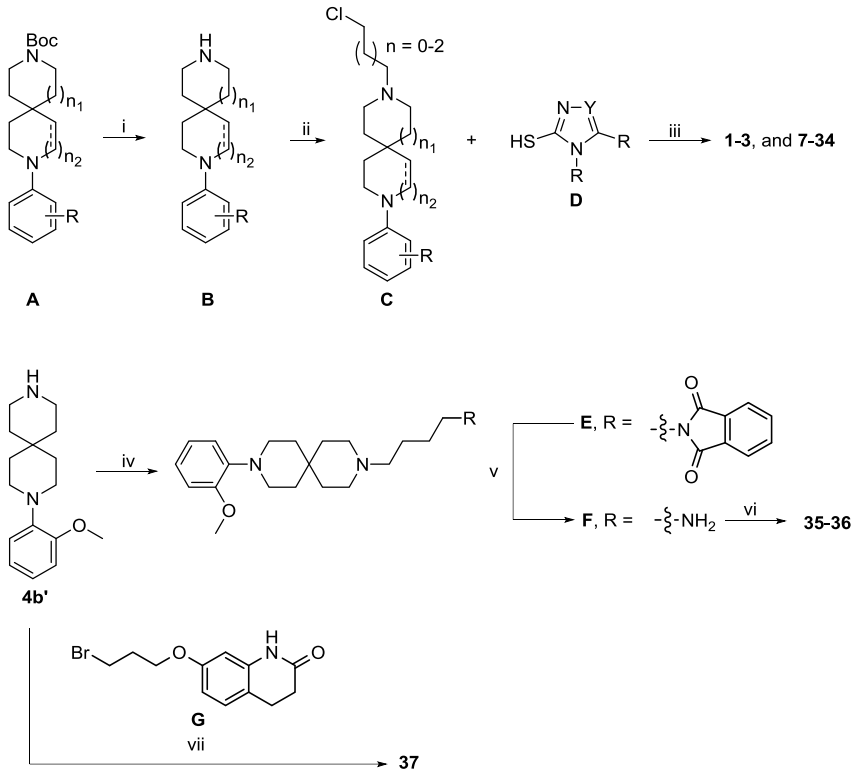

[a]Reagents and conditions: (i) **A**, TFA, CH_2Cl_2, rt, 3 h; (ii) **B**, alkylating reagent, K_2CO_3, acetone, rt, 12 h; (iii) **C**, **D**, TEA, EtOH, 75 °C, 12 h; (iv) **4b'**, 2-(4-bromobutyl)isoindoline-1,3-dione, KI and Cs_2CO_3, ACN, 75 °C for 3 h; (v) **E**, hydrazine, EtOH, 75 °C for 2 h; (vi) **F**, benzoic acid, HOBt, EDC, CH_2Cl_2, rt, 2 h; (vii) **G**, KI, and K_2CO_3, ACN, 90 °C for 12 h.

Radioligand Binding Profiles of Compound 1 Analogues and Fragments. Structural modifications were made to **1** in attempts to further enhance D_3R binding affinity and probe the structural

determinants of this ligand template responsible for receptor selectivity. Compounds and synthons of select ligands were then evaluated in radioligand binding assays using [^{125}I]IABN with HEK 293 cells stably expressing human D_3R and D_{2L} (Tables 1-5). Values of cLogP and topological polar surface area (tPSA) are also included in Tables 1-4 to provide an estimate of lipophilicity and cell permeability, respectively, for each full-length ligand.

We first modified the aryl 1,2,4-triazole ring system in **1**, and evaluated several aryl moieties found to be tolerable in azaspirocyclic D_3R ligand architectures previously disclosed by Micheli and co-workers.[18-20] However, we observed a drastic decrease in receptor selectivity after installing the 4-(1,3-oxazol-2-yl)-phenyl (**11**) and cyclohexyl (**14**) substitutions (D_2R/D_3R ratio = 62 and 221, respectively), indicating our 1,2,4-triazole ligand architecture follows a different structure-activity relationship (SAR) within the D_3R. When modifying the aryl ring with fluorine substitutions, we found the *ortho* position to be more preferred (**12**, K_i = 25.9 nM, D_2R/D_3R ratio = 759), as the 4-fluoro analogue resulted in a 2-fold decrease in receptor selectivity (**13**, K_i = 39.8 nM, D_2R/D_3R ratio = 396).

Next, binding profiles of ligands containing structural modifications to the 1,2,4-triazole ring system were evaluated (**15-19**). With respect to **1**, replacing the $–CH_3$ group for a $–CH_2CH_3$ (**15**) or $–NH_2$ (**16**) substituent resulted in a 7-fold and 5-fold decrease in receptor selectivity, respectively. Similarly, deletion of the $–CH_3$ group resulted in drastic loss of receptor selectivity, affording a 35-fold D_2R/D_3R ratio for **17**, combined with a moderate decrease in D_3R affinity (K_i = 32.5). Imidazole systems were also evaluated as triazole alternatives, however, we found a significant loss in receptor affinity and binding selectivity for ligands **18** and **19**.

Table 1. D_3R/D_2R Binding Profiles of 1 Analogues with Modifications to the 1,2,4-Triazole System[a]

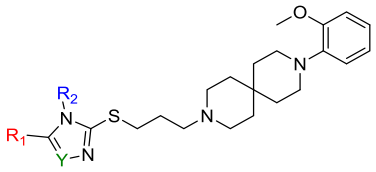

Compound	R_1	R_2	Y	K_i ± SEM (nM)[b]		D_2/D_3 Ratio[e]	cLogP[f]	tPSA[f]
				D_3R[c]	D_2R[d]			
1[g]	phenyl	CH_3	N	12.0 ± 2.8	10,895 ± 2,069	905	4.88	43.67
7	4-*N*,*N*-dimethylaniline	CH_3	N	138 ± 17.1	12,137 ± 2,713	88	5.21	46.91
8	2-methoxyphenyl	CH_3	N	63.0 ± 7.5	2,112 ± 269	33.5	4.37	52.90
9	pyrimidin-3-yl	CH_3	N	213 ± 21.4	48,584 ± 10,378	229	3.69	56.03
10	4-(thiophen-3-yl)phenyl	CH_3	N	101 ± 32.3	3,250 ± 782	32.2	6.41	43.67
11	4-(1,3-oxazol-2-yl)-phenyl	CH_3	N	25.4 ± 2.7	1,574 ± 396	62.1	4.66	65.26
12	2-fluorophenyl	CH_3	N	25.9 ± 3.7	19,655 ± 4,441	759	5.03	43.67
13	4-fluorophenyl	CH_3	N	39.8 ± 11.9	15,768 ± 1,661	396	5.03	43.67
14	cyclohexyl	CH_3	N	57.0 ± 13.6	12,584 ± 1,732	221	5.17	43.67
15	phenyl	CH_2CH_3	N	48.7 ± 8.9	5,650 ± 893	116	5.55	43.67
16	phenyl	NH_2	N	75.0 ± 6.3	13,904 ± 453	185	4.90	69.69
17	phenyl	H	N	32.5 ± 2.6	1,162 ± 229	35.7	5.06	52.46
18	phenyl	H	CH	383 ± 53.7	5,891 ± 267	15.4	6.24	40.1
19	phenyl	CH_3	CH	418 ± 49.8	3,5720 ± 5,804	85.4	6.26	31.21

[a]Spiperone assayed under the same conditions as a reference blocker: D_2R, 0.06 ± 0.001 nM; D_3R, 0.33 ± 0.02 nM; D_4R, 0.45 ± 0.01 nM. [b]Mean ± SEM; K_i values were determined by at least three experiments. [c]K_i values for D_3 receptors were measured using human D_3 expressed in HEK cells with [^{125}I]IABN as the radioligand. [d]K_i values for D_2 receptors were measured using human D_2 expressed in HEK cells with [^{125}I]IABN as the radioligand. [e](K_i for D_2 receptors)/(K_i for D_3 receptors). [f]Calculated using ChemDraw Professional 15.1. [g]Compound reported in our initial work ref. 14.

We then explored the effect on D_3R binding by manipulating the linker length in compounds **20** and **21** (Table 2). However, this modification afforded an ~8-fold reduction in D_3R selectivity, demonstrating the *N*-propyl linker to be the more optimal spacer. Next, we probed the influence of the 2-methoxy substituent in compound **1** on D_3R ligand binding. When replacing the 2-methoxy with a 2-ethoxy in **22**, receptor selectivity was diminished (D_2R/D_3R ratio = 114), along with a moderate decrease in binding affinity (K_i = 45.1 nM). Compared to **20**, the 2-fluoroethoxy substituent showed to be more compatible, affording an increase in overall binding and selectivity (K_i = 33.3 nM, D_2R/D_3R ratio = 192). In our initial report, we found moving the aryl methoxy substituent from the 2-position in **1** to the 4-position in **25** further enhanced D_3R selectivity (D_2R/D_3R ratio = ~1,000-fold), but also diminished ligand affinity for the receptor (K_i = 97.7 nM).[14] Thus, we evaluated **26**, a compound containing methoxy substituents in the *ortho* and *para* positions of the aryl ring, to determine if affinity could be enhanced while maintaining similar selectivity. Instead, we found the receptor affinity for **26** (K_i = 112 nM) to be comparable to **25**, along with a ~2-fold reduction in D_3R selectivity (D_2R/D_3R ratio = 584).

Next, we examined the binding profiles of fluorinated derivatives **28-30**. When moving the fluorine atom from the 4-position (**27**) to the 2-position in **28**, a loss in receptor affinity (K_i = 208 nM) and selectivity (D_2R/D_3R ratio = 126) is observed. Upon installing a $-CF_3$ functional group in the *para* position of the aryl ring in **29**, we observed a further decrease in both D_3R affinity (K_i = 370 nM) and selectivity (D_2R/D_3R ratio = 57). Due to the excellent D_3R binding properties observed with compounds **1** and **27**, we evaluated the 4-fluoro-2-methoxyphenyl ring system in ligand **30**. Compared to **1**, compound **30** was found to have a comparable D_3R binding affinity (K_i = 21.0 nM) to **1**, along with a modest improvement in receptor selectivity (D_2R/D_3R ratio = 934).

Table 2. D_3R/D_2R Binding Profiles of 1 Analogues with Modifications to the Linker and Aryl Ring[a]

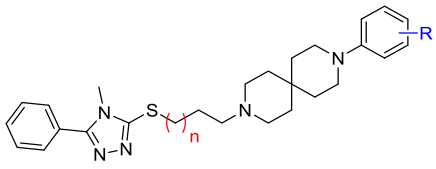

Compound	n	R	K_i ± SEM (nM)[b]		D_2/D_3 Ratio[e]	cLogP[f]	tPSA[f]
			D_3R[c]	D_2R[d]			
20	0	2-methoxy	89.7 ± 22.5	9,004 ± 1,133	100	4.54	43.67
21	2	2-methoxy	59.2 ± 5.1	9,248 ± 1,745	156	5.06	43.67
22	1	2-ethoxy	45.1 ± 9.7	5,165 ± 525	114	5.41	43.67
23	1	2-hydroxy	396 ± 17.3	17,595 ± 4,185	44.4	4.33	54.67
24	1	2-fluorethoxy	33.3 ± 1.7	6,379 ± 964	192	5.27	43.67
25[g]	1	4-methoxy	97.7 ± 17.4	104,847 ± 29,076	1,073	4.88	43.67
26	1	2,4-dimethoxy	112 ± 24.5	65,229 ± 37,252	584	4.89	52.90
27[g]	1	4-fluoro	25.6 ± 5.6	9,792 ± 1,790	383	5.32	34.44
28	1	2-fluoro	208 ± 9.6	26,253 ± 6,866	126	5.32	34.44
29	1	2-fluoro-4-trifluoromethyl	370 ± 17.8	21,172 ± 1,499	57.2	6.38	34.44
30	1	2-methoxy-4-fluoro	21.0 ± 1.4	19,634 ± 3,691	934	5.17	43.67

[a]Spiperone assayed under the same conditions as a reference blocker: D_2R, 0.06 ± 0.001 nM; D_3R, 0.33 ± 0.02 nM; D_4R, 0.45 ± 0.01 nM. [b]Mean ± SEM; K_i values were determined by at least three experiments. [c]K_i values for D_3 receptors were measured using human D_3 expressed in HEK cells with [^{125}I]IABN as the radioligand. [d]K_i values for D_2 receptors were measured using human D_2 expressed in HEK cells with [^{125}I]IABN as the radioligand. [e](K_i for D_2 receptors)/(K_i for D_3 receptors). [f]Calculated using ChemDraw Professional 15.1. [g]Compound reported in our initial work ref. 14.

Next, we evaluated two additional analogues containing modified diazaspiro cores (Table 3). In contrast to **1** and **31**, unsaturated ligand **32**, containing a novel diazaspiro[5.5]undec-1-ene amino core, was found bind with higher affinity at the D_3R (K_i = 3.2 nM), although receptor selectivity was not maintained (D_2R/D_3R ratio = 60). Interestingly, when reversing the diazaspiro[4.5]decane moiety found

in **33**, a two-fold increase in receptor selectivity was observed for ligand **34** (D_2R/D_3R ratio = 758), along with a similar D_3R binding affinity (K_i = 27.8 nM).

Table 3. D_3R/D_2R Binding Profiles of 1 Analogues with Modifications to the Amino Core[a]

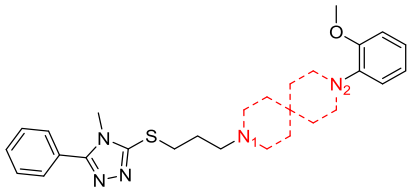

Compound	Amino Core	K_i ± SEM (nM)[b]		D_2/D_3 Ratio[e]	cLogP[f]	tPSA[f]
		D_3R[c]	D_2R[d]			
31[g]		6.5 ± 0.88	260 ± 44.2	40.2	4.09	43.67
32	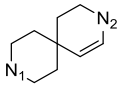	3.2 ± 0.71	197 ± 24.4	60.7	5.38	43.67
33[g]	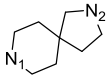	19.6 ± 4.7	6,168 ± 939	315	4.32	43.67
34	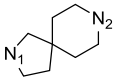	27.8 ± 4.4	21,098 ± 3,069	758	4.32	43.67

[a]Spiperone assayed under the same conditions as a reference blocker: D_2R, 0.06 ± 0.001 nM; D_3R, 0.33 ± 0.02 nM; D_4R, 0.45 ± 0.01 nM. [b]Mean ± SEM; K_i values were determined by at least three experiments. [c]K_i values for D_3 receptors were measured using human D_3 expressed in HEK cells with [^{125}I]IABN as the radioligand. [d]K_i values for D_2 receptors were measured using human D_2 expressed in HEK cells with [^{125}I]IABN as the radioligand. [e](K_i for D_2 receptors)/(K_i for D_3 receptors). [f]Calculated using ChemDraw Professional 15.1. [g]Compound reported in our initial work ref. 14.

Finally, we evaluated the diazaspiro[5.5]undecane amino core in two aryl amide templates that were previously identified as excellent D_3R-prefering scaffolds when conjugated to the 1-(2-methoxyphenyl)piperazine system (Table 4).[21, 22] While maintaining the 2-methoxyphenyl aryl system,

we investigated 4-(dimethylamino)- and 4-(thiophen-3-yl)-benzamides with a four carbon spacer linked to the diazaspiro[5.5]undecane moiety. However, using this ligand framework, compounds **35** and **36** both exhibited poor D_3R receptor affinity and selectivity. This diazaspiro core was then evaluated in a D_2R-prefering aripiprazole ligand architecture disclosed in our previous work.[17] Although **37** appears to be slightly D_2R-selective, receptor affinity was low.

Table 4. D_3R/D_2R Binding Profiles of 1 Analogues with Modifications to the Aryl Head Group[a]

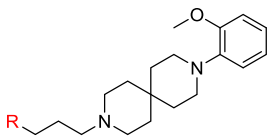

Compound	R	$K_i \pm$ SEM (nM)[b]		D_2R/D_3R Ratio[e]	cLogP[f]	tPSA[f]
		D_3R[c]	D_2R[d]			
35	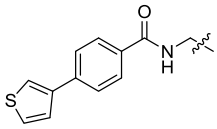	92.9 ± 20.5	2,766 ± 582	29.8	5.64	44.81
36	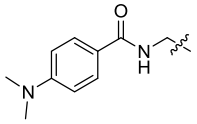	61.5 ± 15.0	3,762 ± 776	61.2	4.43	48.05
37	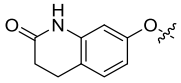	14,587 ± 1,772	2,630 ± 400	0.1	4.50	54.04

[a]Spiperone assayed under the same conditions as a reference blocker: D_2R, 0.06 ± 0.001 nM; D_3R, 0.33 ± 0.02 nM; D_4R, 0.45 ± 0.01 nM. [b]Mean ± SEM; K_i values were determined by at least three experiments. [c]K_i values for D_3 receptors were measured using human D_3 expressed in HEK cells with [^{125}I]IABN as the radioligand. [d]K_i values for D_2 receptors were measured using human D_2 expressed in HEK cells with [^{125}I]IABN as the radioligand. [e](K_i for D_2 receptors)/(K_i for D_3 receptors). [f]Calculated using ChemDraw Professional 15.1.

Lead compound **1** was fragmented in order to identify synthons acting as primary (PP) or secondary pharmacophores (SP). Unexpectedly, fragments **4b'** and **5a** were found to have micromolar

affinity for the receptor, with **5a** exhibiting nominal D_3R selectivity (Table 5). Low receptor binding was also observed with synthons **5b** and **5c**, despite the K_i values of 19.6 nM and 24.2 nM obtained from the parent compounds **2** and **3**, respectively. The binding affinities obtained with **5a-c** are in contrast to those reported for alkylated arylpiperazine synthons (i.e., **5d**[11] and **5e**[21, 23]) of potent D_3R ligand scaffolds. These PP typically show K_i values of ~ 10-20 nM at the receptor by engaging the orthosteric binding pocket (OBP) of the protein. This allows the ionizable nitrogen of these PP to form an ionic interaction with the highly conserved Asp110 [3.32] residue within the OBP, affording the favorable receptor affinity of these orthosteric fragments.

Binding studies continued with evaluation of synthons from the right-half of lead compound **1** to determine if receptor affinity was being engaged by an unexpected 1,2,4-triazole pharmacophore. Similar to the displacement observed with synthon **5a**, low receptor binding was observed with fragments **6a**, **6c**, **6d**, and **6f**. Although minimal potency was observed with these 1,2,4-trizole synthons, a trend of increasing affinity was observed when elongating fragment **6a** with piperdine (**6c**), and 4,4-dimethylpiperidine (**6d**). In addition, we found **6f** to be ~197-fold selective for the D_3R over the D_2R, while piperazine analogue **6h** illustrated no receptor selectivity. We hypothesized the 1,2,4-triazole system may be key in directing, and subsequently, stabilizing the bulky diazaspiro PPs of **1-3**, within the OBP of the receptor. Once stabilized, these diazaspiro systems may be able to interact with residues within the OBP due to the large structural space these systems inhabit which are not accessible to the piperazine PP of **31**.

Table 5. D_3R/D_2R Binding Profiles of Synthons[a]

Compound	Synthon	$K_i \pm$ SEM (nM)[b]		D_2R/D_3R Ratio[e]	Compound	Synthon	$K_i \pm$ SEM (nM)[b]		D_2R/D_3R Ratio[e]
		D_3R[c]	D_2R[d]				D_3R[c]	D_2R[d]	
4b'	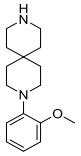	>39,319 ± NA	99,379 ± 11,752	>2.5	**6a**	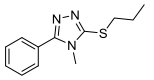	>50,316 ± NA	180,375 ± 70,719	>3.6
5a	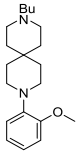	2,773 ± 384	26,739 ± NA	>9.6	**6c**	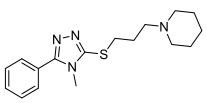	1,098 ± 53.8	98,462 ± 18,965	89.6
5b	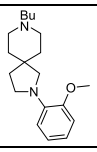	6,647 ± 4,559	25,823 ± 14,830	3.9	**6d**	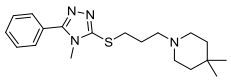	631 ± 43.7	59,994 ± 22,704	95.1
5c	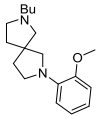	23,256 ± 9,615	26,050 ± NA	>1.1	**6f**	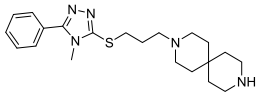	1,145 ± 97.1	>225,748 ± NA	>197
5d[f]	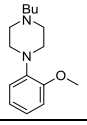	23.9 ± 5.8	20.6 ± 4.8	0.86	**6h**	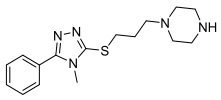	72,753 ± 13,438	74,272 ± 17,815	1
5e	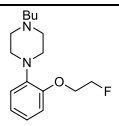	14.7 ± 1.2	22.3 ± 4.9	1.5					

[a]Spiperone assayed under the same conditions as a reference blocker: D_2R, 0.06 ± 0.001 nM; D_3R, 0.33 ± 0.02 nM; D_4R, 0.45 ± 0.01 nM. [b]Mean ± SEM; K_i values were determined by at least three experiments. [c]K_i values for D_3 receptors were measured using human D_3 expressed in HEK cells with [^{125}I]IABN as the radioligand. [d]K_i values for D_2 receptors were measured using human D expressed in HEK cells with [^{125}I]IABN as the radioligand. [e](K_i for D_2 receptors)/(K_i for D_3 receptors). [f]Compound and receptor binding data from ref. 11.

Molecular Docking Studies. To probe these potential protein-ligand interactions, select compounds were modeled within the D_3R (3PBL) to identify residue contacts within orthosteric and SBP of the receptor (**Figure 2**, **A**). A top docking pose of **1** was found to engage in multiple polar and non-polar contacts between the arylated diazaspiro[5.5]undecane moiety, including π–π stacking interactions between the aryl ring and the Phe346$^{6.52}$ residue within the OBP of the receptor (**Figure 2**, **B**). Similarly,

ligand docking also predicted the diazaspiro[5.5]undecane moiety of ligand **17**, and diazaspiro[5.5]undec-1-ene system of high-affinity compound **32**, to also engage in hydrophobic interactions with residues Phe346 [6.52] and Phe345 [6.51] (**Figure 2**, **C** and **F**). When evaluating the potential salt bridge formation between residue Asp110 [3.32] and the ionizable nitrogens in the diazaspiro cores of scaffolds **1**, **17**, and **32**, we identified distances of 3.4 Å, 3.2 Å and 3.1 Å, respectively. Interestingly, these were all found to be greater than the predicted 2.7 Å distance observed with binding pose of compound **31** (**Figure 2, E**). These results could explain the contrasting receptor binding affinity observed between diazaspiro PP **5a** and piperazine PP **5d**. Thus, we surmise the 1,2,4-triazole side of the molecule appropriately positions the bulky diazaspiro[5.5]undecane moiety within the hydrophobic cavity of the D_3R OBP, allowing the amino core to engage in non-polar interactions with residues Phe346 [6.52] and Phe345 [6.51]. These contacts then assist in stabilizing this "weaker" ionic interaction with Asp110 [3.32], resulting in the observed receptor affinity for **1**, **17**, and **32**. This analysis is also consistent with the poor binding affinity for compound **19**, as the docking pose predicted minimal hydrophobic interactions with residues Phe345 [6.52] and Phe346 [6.51], and a distance of 4.2 Å between the protonated nitrogen of the ligand and the conserved Asp110 [3.32] side chain (**Figure 2**, **D**).

Next, we evaluated interactions between the non-conserved residues within the SBP of the D_3R, responsible for ligand selectivity,[11] and the predicted binding modes of **1** and its derivatives. In addition to the significant polar and non-polar interactions between Val86 [2.61] and the 1,2,4-triazole system of lead compound **1**, we also identified a potential weak hydrogen bond interaction between Glu90 [2.65] and the methyl substituent of the *N*-heterocycle (**Figure 2**, **B**). Disruption of this C–H···O interaction may explain the reduction in receptor selectivity for compound **17** (**Figure 2**, **C**), in which the only structural difference between this ligand and **1**, is the removal of the $–CH_3$ group. When substituting the $–CH_3$ with $–CH_2CH_3$ (**15**) or $–NH_2$ (**16**), receptor selectivity is again diminished, while binding affinity is moderately maintained. Although the N–H···O hydrogen bond interactions of **17** and Glu90 [2.65] would appear to be more favorable than the C–H···O interactions of **1**, previous studies have shown the latter to result in

more favorable binding profiles due to the potential penalty associated with $-NH_2$ desolvation upon ligand binding.[24, 25]

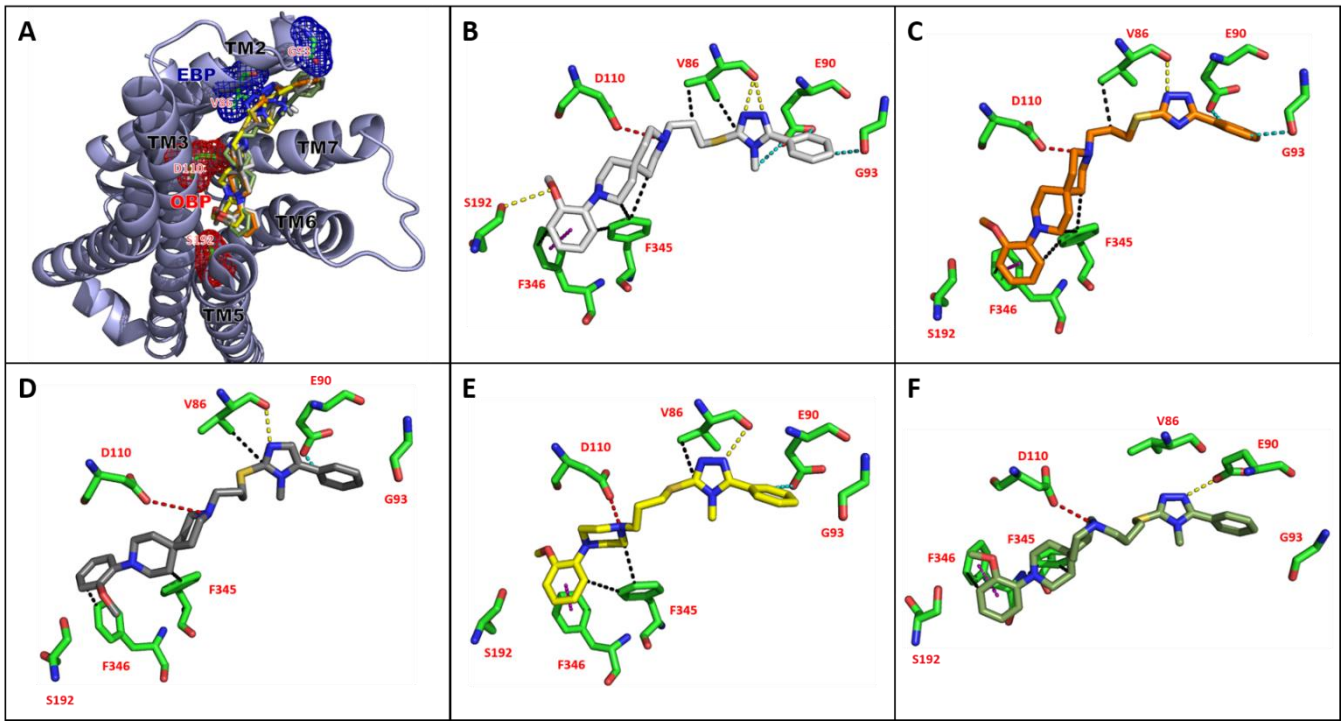

Figure 2. (**A**) Predicted binding modes of compound **1** derivatives in complex with the D_3R (3PBL). Predicted polar (yellow, 3.0 Å cut-off), weak hydrogen bonding (magenta, 3.6 Å cut-off), π–π stacking (purple, 5.5 Å cut-off), and hydrophobic (black, 4.0 Å cut-off) residue interactions with compounds **1** (**B**), **17** (**C**), **19** (**D**), **31** (**E**), and **32** (**F**) within the binding pocket of the receptor. Interaction between the Asp110 [3.32] residue and the ionizable nitrogen of the ligand scaffold is shown in red.

Previous reports have discussed the critical role EL1 Gly residues can play in determining D_2R/D_3R selectivity of ligands.[26, 27] Glycine can act as an acceptor in weak hydrogen bond interactions in many protein-ligand complexes.[24] In our study, the predicted binding pose of **1** places the aryl ring off of the 1,2,4-triazole moiety in close proximity to the Gly93 [EL1] residue, affording potential weak C–H···O interactions. However, this interaction is found to be absent in the binding poses of less selective ligands **31** and **32**. We hypothesize the lack of receptor selectivity observed for compounds **10-11** and **13** may be a result of steric clashing between the *para* substituents of these ligands and the Gly93 [EL1] residue in

the SBS. This steric clash could also explain the lack of receptor selectivity for compounds **21** and **35-36**, which all contain a butyl spacer group, compared the shorter propyl linker of **1**. We observed this proposed SAR trend after installing a C–F bond in the *para* position of **1**, resulting in a loss of receptor selectivity for **13** (D_2R/D_3R = 905 vs. 396, respectively). Receptor selectivity was able to be slightly restored, however, after moving the C–F substitution to *ortho* site of the aryl ring in **12**, potentially alleviating steric interactions afforded with Gly93 [EL1] and compound **13**.

Compound 1 Competitively Inhibits DA at the OBP. To confirm the binding mode of **1** does indeed require occupancy within the OBP, we evaluated **1** (**Figure 3**, **A**), **31** (**Figure 3**, **B**), and known allosteric modulator SB269652[28, 29] (**Figure 3**, **C**) in a *β*-arrestin assay with endogenous ligand dopamine (DA) as the orthosteric ligand. Both **1** and **31** caused a limitless rightward shift in the dopamine-dose response curves, suggesting a competitive mode of action at the OBP.[30] This is in contrast to the limited dextral shift that is observed with SB269652, resulting from the allosteric pharmacology of the compound at the receptor. Furthermore, when plotting the concentration-response (CR) curves for **1** and SB269,652 into a Schild plot, a linear regression slope near unity is obtained for **1**, indicative of competitive antagonism,[31] while a non-linear regression slope is observed for SB269,652, indicating an allosteric mode of antagonism (See SI).[32-34] Overall, these data clearly indicate **1** behaves in a competitive manner at the OBP with the orthosteric endogenous ligand DA, ruling out an allosteric binding mechanism for the diazaspiro ligand.

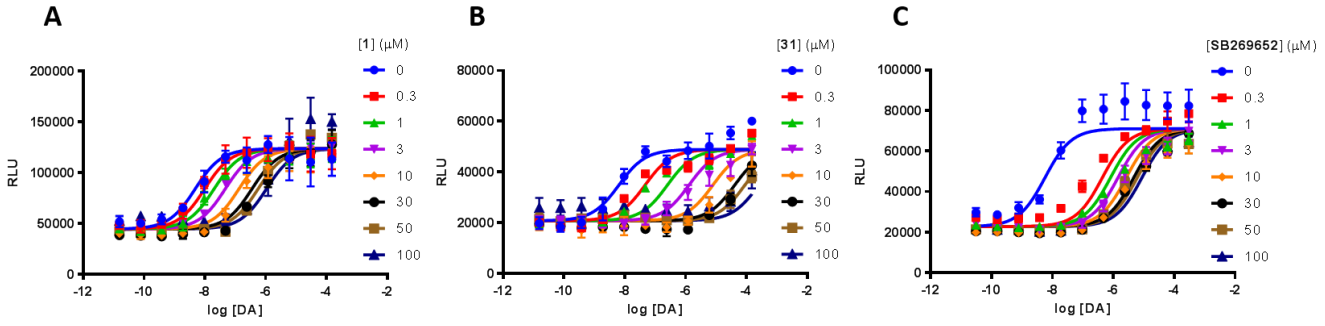

Figure 3. Curve shift analysis of **1** (**A**), **31** (**B**), and SB269,625 (**C**) using a dopamine (DA) mediated *β*-arrestin 2 recruitment assay. The receptor was stimulated with the indicated concentration of DA along with and without concentrations of the test compound. Data points represent the mean ± SEM of dopamine-induced luminescence response obtained from seven to sixteen replicates.

PDSP Pharmacological Evaluation. Compounds **1** and **31** were then submitted to the Psychoactive Drug Screening Program (PDSP)[35, 36] to evaluate the binding (Table 6) and functional behavior of the ligands at D_1- and D_2-like receptors (**Figure 4**). Compared to our initial report, the PDSP obtained K_i values that differed slightly from our initial report[14] for both compounds at the D_3R and D_2R. However, this is most likely due to the use of [^{3}H]*N*-methylspiperone by the PDSP in their binding assay, compared to our use of [^{125}I]IABN, a high-affinity radioligand with negligible non-specific binding[37]. Compound **1** showed no interaction at the D_4R or D_1-like receptors, while **31** exhibited K_i values of 721 nM and ~ 3 μM at the D_4R and D_5R, respectively (Table 6). Lead compound **1** was found to behave as a preferential D_3R antagonist (IC_{50} = 41.4 nM) with negligible functional potency at the D_2R (IC_{50} > 1.5 μM) (**Figure 4, D**). While antagonist affinities are known to vary depending on the competing agonist used[38], we are currently evaluating **1** in other cell-signaling cascade models to further assess the 39-fold D_2R/D_3R selectivity ratio observed in the PDSP Tango functional assays. Ligand **31** however, was found to be a weak agonist/antagonist at both the D_2R and D_3R (**Figure 4, C-F**), a common nuance that has been disclosed with previously reported D_3R selective piperazine-based scaffolds.[11, 39] This can be attributed to the lack of receptor selectivity that is engaged with the aryl piperazine orthosteric PP of the ligand scaffold. Finally, compound **31** was also identified as a weak partial agonist at the D_4R (IC_{50} = 427 nM) (**Figure 4, G**).

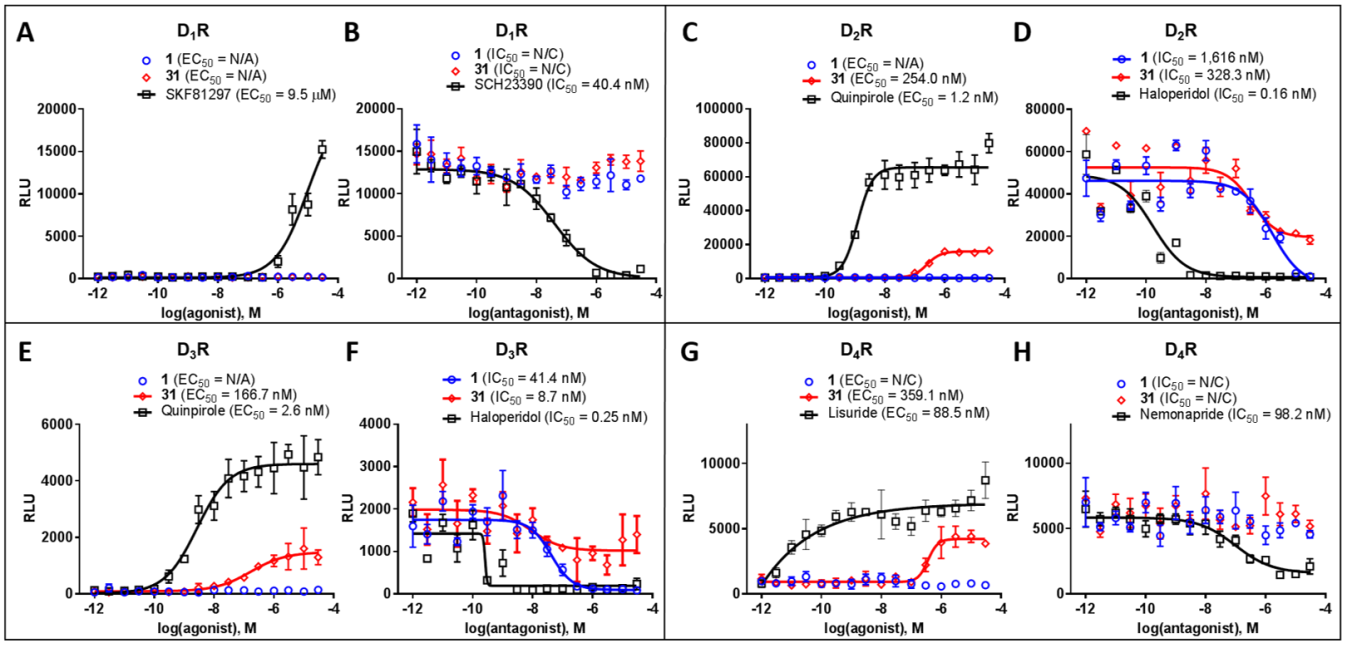

Figure 4. Agonist and antagonist selectivity profiling with G-protein-independent *β*-arrestin recruitment Tango assays at human D_1- and D_2-like receptors. (**A**) Concentration-response to varying doses of D_1R agonists and control SKF81297. (**B**) Response to varying doses of D_1R antagonists and control SCH23390, added 30 min before addition of a final EC_{80} concentration (3 μM) of reference agonist SKF81297. (**C**) Concentration-response to varying doses of D_2R agonists and control quinpirole. (**D**) Concentration-response to varying doses of D_2R antagonists and control haloperidol, added 30 min before addition of a final EC_{80} concentration (3 nM) of reference agonist quinpirole. (**E**) Concentration-response to varying doses of D_3R agonists and control quinpirole. (**F**) Concentration-response to varying doses of D_3R antagonists and control haloperidol, added 30 min before addition of a final EC_{80} concentration (3 nM) of reference agonist quinpirole. (**G**) Concentration-response to varying doses of D_4R agonists and control lisuride. (**H**) Concentration-response to varying doses of D_4R antagonists and control nemonapride, added 30 min before addition of a final EC_{80} concentration (100 nM) of reference agonist lisuride. Data are shown as mean ± SEM of 3 independent experiments. N/A, not active. N/C, data not converged.

PDSP also evaluated compounds **1** and **31** for off-target interactions with other GPCRs (Table 6). Similar to the findings in our initial publication[14], ligand **31** was found to bind with high affinity at the 5-

HT_{1A} (K_i = 0.9 nM) and 5-HT_{2B} (K_i = 42 nM) receptors, and was also found to exhibit marginal inhibitions at the 5-HT_{2C} (K_i = 159 nM) and 5-HT_{7A} (K_i = 128 nM). Compound **1**, however, exhibited negligible affinities (K_i > 1 μM) for all the serotonin subclass receptors in the study. These findings show the potential of **1** as a D_3R PET agent, as serotoninergic interactions are known to hinder many piperazine containing scaffolds[40-42, 23, 43].

Among the subclass of histamine GPCRs screened, both compounds bind at the H_1 histamine receptor, with high affinity (**1,** K_i = 8 nM; **31**, K_i = 40 nM). No appreciable opioid receptor inhibition was identified during the primary screen for **1** and **31** at 10 μM drug concentrations. Lead compound **1** was found to weakly interact at the muscarinic M_1 (54% inhibition at 10 μM of compound) and M_3 (K_i = 514 nM) receptors as well.

Off-target interactions were discovered with compounds **1** and **31** at the subfamilies of the α_1- and α_2-adrenergic receptors, which are GPCRs known to play a role in vasoconstriction.[44] While **1** showed no appreciable interactions at the examined adrenergic sites, compound **31** was found to be active at the α_{1A} (K_i = 49 nM) and the α_{1B} (K_i = 94 nM) receptors, with moderate inhibitive action at the α_2 subclass group. Adrenergic interactions have been observed with many piperazine-containing D_3R ligand scaffolds[45], including BP 897.[46] This is consistent with a recent study indicating α_2-adrenoceptors are targets for known D_2-like receptor ligands including 7-OH-PIPAT, RO-105824, and dopamine.[47] Unsurprisingly, the liability of D_3R antagonists to induce hypertension, observed with GSK598809 in dog models[48], has hindered these class of compounds from progressing in clinical trials as potential addiction therapeutics[49], making the selective nature of **1** over the adrenergic receptors particularly encouraging.

Table 6. Binding Affinities of Compounds 1 and 31 at Select GPCRs[a]

GPCR		K_i (nM)[a] or % Inhibition at 10 μM[b]		GPCR		K_i (nM)[a] or % Inhibition at 10 μM[b]	
		1	**31**			**1**	**31**
Dopamine	D_1	N/A	N/A	**Muscarinic**	M_1	54%	N/A
	D_2	N/A	577		M_2	52	N/A
	D_3	94	6		M_3	514	NT
	D_4	N/A	721		M_4	590	N/A
	D_5	N/A	3,016		M_5	N/A	N/A
Serotonin	5-HT_{1A}	1,297	0.9	**Adrenergic**	α_{1A}	2,178	49
	5-HT_{1B}	N/A	2,032		α_{1B}	2,173	94
	5-HT_{1D}	N/A	>50%		α_{2A}	N/A	221
	5-HT_{1E}	N/A	N/A		α_{2B}	N/A	241
	5-HT_{2A}	N/A	1,415		α_{2C}	1,557	433
	5-HT_{2B}	2,144	42		$\alpha_2\beta_2$	N/A	N/A
	5-HT_{2C}	N/A	159		$\alpha_2\beta_4$	N/A	N/A
	5-HT_3	N/A	N/A		$\alpha_3\beta_2$	N/A	N/A
	5-HT_{5A}	N/A	N/A		$\alpha_3\beta_4$	8,523	N/A
	5-HT_6	N/A	N/A		$\alpha_4\beta_2$	N/A	N/A
	5-HT_{7A}	N/A	128		$\alpha_4\beta_4$	N/A	N/A
Histamine	H_1	8	40		β_1	N/A	N/A
	H_2	NT	NT		β_2	N/A	60%
	H_3	73%	N/A		β_3	N/A	N/A
	H_4	N/A	N/A	**Dopamine Active Transporter (DAT)**		N/A	N/A
Opioid	μ	N/A	N/A	**Norepinephrine Transporter (NET)**		931	N/A
	κ	N/A	N/A	**Serotonin Transporter (SERT)**		295	N/A
	δ	N/A	N/A	**$GABA_A$**		N/A	N/A

N/A, not active (<50% inhibition obtained in primary assay at 10 μM of compound). NT, not tested. [a]K_i values determined by at least three experiments. [b]% of receptor inhibition at 10 μM of compound, values determined by at least three experiments.

CONCLUSIONS

In our previous report, we identified **1** as a new lead D_3R selective compound containing a novel diazaspiro[5.5]undecane amino core.[14] In this study, we imposed structural modification to **1**, affording

analogues with slightly enhanced D_3R selectivity (**30**, D_3R K_i = 21.0 nM, D_2R/D_3R ratio = 934) and affinity (**32**, D_3R K_i = 3.2 nM, D_2R/D_3R ratio = 60). Fragmentation of **1** revealed diazaspiro[5.5]undecane synthon **5a** to be a low-affinity PP for the receptor (**5a**, D_3R K_i > 2.7 μM), despite the excellent potency observed with the full length compound (**1**, D_3R K_i = 12.0 nM). Molecular docking studies predicted the 1,2,4-triazole half of **1** to favorably position the bulky diazaspiro within the OBP of the receptor, allowing the amino core to engage in hydrophobic interactions with the Phe345 [6.52] and Phe346 [6.51] residues, ultimately stabilizing the "weak" ionic interaction between the ionizable nitrogen of the PP and the highly conserved Asp110 [3.32]. To verify **1** was not interacting at another receptor site, (i.e., allosteric behavior) we utilized a dopamine-mediated *β*-arrestin 2 recruitment assay to show the competitive manner in which **1** behaves with the orthosteric ligand, revealing the binding mode of **1** does indeed require OBP occupancy. Upon examining the functional behavior of compounds **1** and **31** at D_1- and D_2-like receptors, we found **1** to be a more D_3R selective ligand for both receptor binding and cell signaling. These results, combined with the minimal off-target interactions observed with **1** at other GPCRs, suggests the unique binding contacts between the PP of **1** and the highly conserved residues within OBP of the D_3R receptor play a pivotal role in diminishing non-specific ligand binding with other closely related serotoninergic and adrenergic sites. As such, installing low affinity amino fragments, such as **5a**, into D_3R ligand systems may be beneficial in overcoming drug promiscuity, commonly encountered with piperazine-based ligand scaffolds. This unorthodox approach could be exploited for the development of clinically viable D_3R selective compounds for addiction therapeutic and PET imaging applications.

EXPERIMENTAL SECTION

Chemistry: Arylated amine synthons **4** and **A**-**B** were synthesized following our previously disclosed Pd-catalyzed C–N cross-coupling reports.[15, 16] Compounds **C**, **G**, **6b**, **1-3**, **25**, **27**, **31**, and **33** were obtained following the synthetic procedures outlined in our initial publication.[14] Finally, 1,2,4-triazole compounds **D**, and all other commercial reagents were purchased and used as without further purification. However, **D** analogues were also able to be obtained in good yield following the protocol described by Micheli and

co-workers.[18] NMR spectra were taken on a Bruker DMX 500 MHz. Compound structures and identity were confirmed by ^{1}H and ^{13}C NMR, and mass spectrometry. Compound purity greater than 95% was determined by LCMS analysis using a 2695 Alliance LCMS. Purification of organic compounds were carried out on a Biotage Isolera One with a dual wavelength UV−Vis. detector. Chemical shifts (δ) in the NMR spectra (^{1}H and ^{13}C) were referenced by assigning the residual solvent peaks. Compounds were taken up with CH_2Cl_2 followed by dropwise addition of a 2.0 M HCl solution in diethyl ether. After stirring at room temperature for 1 h, the solvent was removed under reduced pressure to afford the desired compound as a hydrochloride salt for *in vitro* studies.

General Method A: Synthesis of Fragmented Synthons 4-5. The appropriate arylated diazaspiro and piperazine precursors (**4**), obtained following our previous reports,[15, 16] were dissolved in CH_2Cl_2 (2 mL), followed by dropwise addition of CF_3COOH (2 mL), and stirred at room temperature for 3 h. Volatiles were then removed under reduced pressure and the crude product was neutralized with a saturated $NaHCo_{3(aq)}$ solution (10 mL). The reaction mixture was extracted with CH_2Cl_2 (3 x 20 mL), and the organic layers were combined, dried, and concentrated to afford the free-amine intermediates (**4'**) which were used without further purification. A mixture of **4'** (1.0 mmol), 1-bromobutane (1.1 mmol), and K_2CO_3 (1.5 mmol) was stirred in acetone (5 mL) at room temperature for 5 h. The crude reaction mixture was then filtered, and solvent was removed under reduced pressure. The residue was purified by flash chromatography on silica gel eluting with MeOH solution/CH_2Cl_2 (1:10) affording target compounds (**5**).

General Method B: Synthesis of Diazaspiro Analogues 1-3 and 7-34. Target compounds can be obtained following the synthetic procedures outlined in our initial.[14] Briefly, the appropriate arylated diazaspiro and piperazine precursors (**A**), obtained following our previous reports,[15, 16] were dissolved in CH_2Cl_2 (2 mL), followed by dropwise addition of CF_3COOH (2 mL), and stirred at room temperature for 3 h. Volatiles were then removed under reduced pressure and the crude product was neutralized with a saturated $NaHCo_{3(aq)}$ solution (10 mL). The reaction mixture was extracted with CH_2Cl_2 (3 x 20 mL), and the organic layers were combined, dried, and concentrated to afford the free-amine intermediates (**B)**

which were used without further purification. A mixture of **B (**1 mmol), alkylating reagent **(**2 mmol), and K_2CO_3 (1.5 mmol) was stirred in acetone (5 mL) at room temperature for 12 h. The crude reaction mixture was then filtered and solvent was removed under reduced pressure. The residue was loaded onto a Biotage SNAP flash purification cartridge and eluded with 5% MeOH in CH_2Cl_2 affording intermediates **C**. Finally, a mixture of **D** (1 mmol), TEA (1.5 mmol), and ethanol (10 mL) was stirred at 75 °C for 15 min. The appropriate intermediate **C** (1 mmol) was then added, and the solution was stirred at 75 °C for 12 h. Solvent from the crude reaction mixture was then removed under reduced pressure. The residue was loaded onto a Biotage SNAP flash purification cartridge and eluded with 10% 7N NH_3 in MeOH solution/CH_2Cl_2 to give the target compounds **1-3** and **7-34**. The residue was loaded onto a Biotage SNAP flash purification cartridge and eluded with 10% 7N NH_3 in MeOH solution/CH_2Cl_2 to give the target compounds **1-3** and **7-34**.

2-(4-(9-(2-Methoxyphenyl)-3,9-diazaspiro[5.5]undecan-3-yl)butyl)isoindoline-1,3-dione (E). 4b' (1 mmol), 2-(4-bromobutyl)isoindoline-1,3-dione (1.2 mmol), KI (1.0 mmol) and Cs_2CO_3 (2.5 mmol) were dissolved in acetonitrile (5 mL), and the reaction mixture was stirred at 75 °C for 3 h. The reaction mixture was then filtered and solvent was removed under reduced pressure. Crude residue was purified by silica gel column chromatography using ethyl acetate/hexane (1:1) as the mobile phase to afford **E** as a light-orange solid (Yield 64%). ^{1}H NMR (500 MHz, $CDCl_3$) δ 7.75-7.74 (m, 2H), 7.62-7.61 (m, 2H), 6.90-6.87 (m, 2H), 6.84-6.82 (m, 1H), 6.77 (d, J = 7.9 Hz, 1H), 3.77 (s, 3H), 3.63 (t, J = 6.9 Hz, 2H), 2.91-2.89 (m, 4H), 2.33-2.28 (m, 6H), 1.62-1.59 (m, 6H), 1.52-1.45 (m, 6H); ^{13}C NMR (125 MHz, $CDCl_3$) δ 168.1, 152.0, 142.0, 133.7, 131.9, 122.9, 122.4, 120.7, 118.0, 110.8, 58.3, 55.1, 49.1, 46.5, 37.6, 35.6, 29.0, 26.5, 24.2; LC-MS (ESI) m/z: 462.64 [M+H]

4-(9-(2-Methoxyphenyl)-3,9-diazaspiro[5.5]undecan-3-yl)butan-1-amine (F). E (1 mmol) and hydrazine hydrate (50-60%) were dissolved in ethanol (5 mL), and the reaction mixture was stirred at 75 °C for 2 h. The reaction mixture was then filtered and solvent was removed under reduced pressure. Crude residue was purified by silica gel column chromatography 10% 7 N NH_3 in MeOH solution/CH_2Cl_2

(1.5:1) to afford **F** as a clear oil (Yield 97%). ^{1}H NMR (500 MHz, $CDCl_3$) δ 6.89-6.86 (m, 2H), 6.82-6.78 (m, 1H), 6.75-6.73 (m, 2H), 3.75 (s, 3H), 2.89-2.87 (m, 4H), 2.62-2.59 (t, *J* = 6.7 Hz, 2H), 2.31 (bs, 4H), 2.26-2.23 (t, *J* = 7.0 Hz, 2H), 1.59-1.1.57 (m, 4H), 1.50-1.49 (m, 4H), 1.46-1.41 (m, 2H), 1.38-1.34 (m, 2H), 1.21 (bs, 2H); ^{13}C NMR (125 MHz, $CDCl_3$) δ 152.0, 142.0, 122.3, 120.6, 117.9, 110.8, 58.8, 55.1, 49.1, 46.5, 41.9, 35.6, 31.7, 28.9, 24.3; LC-MS (ESI) m/z: 332.65 [M+H]

Tert-butyl 9-(2-methoxyphenyl)-3,9-diazaspiro[5.5]undec-7-ene-3-carboxylate (4a). Compound **4a** can be synthesized following using the reaction conditions disclosed in Pd C–N cross-coupling report.[15] Separation of **4a** and the saturated major product **4b** was achieved by flash chromatography on silica gel eluting with a 40% EtOAc/hexane gradient to afford a tan oil. (Yield 9%). ^{1}H NMR (500 MHz, $CDCl_3$) δ 7.02-6.98 (m, 1H), 6.95-6.93 (m, 1H), 6.91-6.86 (m, 2H), 6.28 (d, *J* = 8.1 Hz, 1H), 4.64 (d, *J* = 8.2 Hz, 1H), 3.83 (s, 3H), 3.53-3.50 (m, 2H), 3.46-3.43 (m, 2H), 3.41-3.35 (m, 2H), 1.74-1.72 (m, 2H), 1.54 (bs, 2H), 1.46 (s, 9H), 1.44-1.42 (m, 2H); ^{13}C NMR (125 MHz, $CDCl_3$) δ 155.1, 152.4, 137.6, 132.0, 123.7, 122.2, 121.1, 112.1, 105.5, 79.3, 55.7, 44.2, 39.9, 38.5, 34.5, 30.3, 28.6; LC-MS (ESI) m/z: 303.47 [M-$C(CH_3)_3$+H]

3-Butyl-9-(2-methoxyphenyl)-3,9-diazaspiro[5.5]undecane (5a). Following general method A, **5a** was obtained as a white semi-solid. (Yield 38%). ^{1}H NMR (500 MHz, $CDCl_3$) δ 6.97-6.93 (m, 2H), 6.90-6.88 (m, 1H), 6.83-6.82 (m, 1H), 3.83 (s, 3H), 2.97-2.95 (m, 4H), 2.45 (bs, 4H), 2.38-2.35 (m, 2H), 1.68-1.65 (m, 4H), 1.61-1.59 (m, 4H), 1.52-1.46 (m, 2H), 1.34-1.28 (m, 2H) 0.90 (t, *J* = 7.3 Hz, 3H); ^{13}C NMR (125 MHz, $CDCl_3$) δ 152.3, 142.2, 122.6, 120.9, 118.2, 111.0, 58.8, 55.3, 49.3, 46.7, 35.6, 29.1, 29.0, 20.9, 14.1; LC-MS (ESI) m/z: 317.68 [M+H]

8-Butyl-2-(2-methoxyphenyl)-2,8-diazaspiro[4.5]decane (5b). Following general method A, compound **5b** was obtained as an off-white semi-solid. (Yield 59%). ^{1}H NMR (500 MHz, $CDCl_3$) δ 6.88-6.82 (m, 3H), 6.70 (d, *J* = 7.0 Hz, 1H), 3.80 (s, 3H), 3.37 (t, *J* = 6.9 Hz, 2H), 3.21 (s, 2H), 2.98 (bs, 2H), 2.81-2.78 (m, 2H), 1.99 (bs, 4H), 1.82 (t, *J* = 6.8 Hz, 2H), 1.76-1.73 (m, 2H), 1.38-1.34 (m, 2H), 0.94 (t,

J = 7.3 Hz, 3H); ^{13}C NMR (125 MHz, $CDCl_3$) δ 150.3, 139.2, 121.3, 120.0, 115.3, 112.0, 55.7, 50.5, 48.9, 38.9, 33.3, 26.5, 20.4, 13.7; LC-MS (ESI) m/z: 303.52 [M+H]

2-Butyl-7-(2-methoxyphenyl)-2,7-diazaspiro[4.4]nonane (5c). Following general method A, **5c** was obtained as an oil. (Yield 38%). ^{1}H NMR (500 MHz, $CDCl_3$) δ 6.87-6.80 (m, 3H), 6.68-6.67 (m, 1H), 3.80 (s, 3H), 3.45-3.35 (m, 3H), 3.29 (d, *J* = 9.4 Hz, 1H), 3.12 (bs, 2H), 3.00 (bs, 2H), 2.78-2.75 (m, 2H), 2.07-1.91 (m, 4H), 1.65-1.58 (m, 2H), 1.38-1.33 (m, 2H), 0.92 (t, *J* = 7.3 Hz, 3H); ^{13}C NMR (125 MHz, $CDCl_3$) δ 150.0, 139.1, 121.2, 119.6, 114.8, 112.0, 63.9, 61.8, 56.3, 55.6, 49.6, 47.6, 37.3, 35.7, 29.9, 20.4, 13.8; LC-MS (ESI) m/z: 289.93 [M+H]

1-Butyl-4-(2-(2-fluoroethoxy)phenyl)piperazine (5e). Following general method A, **5e**[50] was obtained as a colorless oil. (Yield 41%). ^{1}H NMR (360 MHz, $CDCl_3$) δ 6.97-6.95 (m, 3H), 6.85 (m, 1H), 4.77 (dt, *J* = 47.5, 4.0 Hz, 2H), 4.25 (dt, *J* = 29.0, 4.0 Hz, 2H), 3.16 (s, 4H), 2.68 (s, 4H), 2.43 (t, *J* = 7.8 Hz, 3H), 1.54 (m, 2H), 1.35 (m, 2H) 0.93 (t, *J* = 7.3 Hz, 3H); ^{13}C NMR (126 MHz, $CDCl_3$) δ 150.9, 141.9, 122.6, 122.1, 118.4, 113.7, 82.5, 81.2, 67.6, 67.4, 58.5, 53.4, 50.3, 28.6, 20.7, 11.9; LC-MS (ESI) m/z: 281.20 [M+H]

4-Methyl-3-phenyl-5-(propylthio)-4H-1,2,4-triazole (6a). A mixture of 4-methyl-5-phenyl-4H-1,2,4-triazole-3-thiol (1.0 mmol), 1-bromobutane (1.1 mmol), and K_2CO_3 (1.5 mmol) was stirred in acetone (5 mL) at room temperature for 12 h. The crude reaction mixture was then filtered, and solvent was removed under reduced pressure. The residue was purified by flash chromatography on silica gel eluting with 10% 7 N NH_3 in MeOH solution/CH_2Cl_2 (1:10) affording **6a** as a white solid. (Yield 81%). ^{1}H NMR (500 MHz, $CDCl_3$) δ 7.58-7.56 (m, 2H), 7.44-7.41 (m, 3H), 3.53 (s, 3H), 3.19 (t, *J* = 7.2 Hz, 2H), 1.78-1.74 (quint, *J* = 7.2 Hz, 2H), 1.00 (t, *J* = 7.3 Hz, 3H); ^{13}C NMR (125 MHz, $CDCl_3$) δ 155.8, 129.9, 128.8, 128.5, 127.1, 35.4, 31.6, 22.9, 13.2; LC-MS (ESI) m/z: 234.17 [M+H]

1-(3-((4-Methyl-5-phenyl-4H-1,2,4-triazol-3-yl)thio)propyl)piperidine (6c). A mixture of **6b**[14] (1.0 mmol), piperdine (1.1 mmol), and Cs_2CO_3 (1.5 mmol) was stirred in acetonitrile (3 mL) at 70 °C for 12

h. The crude reaction mixture was then filtered, and solvent was removed under reduced pressure. The residue was purified by flash chromatography on silica gel eluting with 10% 7 N NH_3 in MeOH solution/CH_2Cl_2 (1:10) affording **6c** as a white solid. (Yield 20%). ^{1}H NMR (500 MHz, $CDCl_3$) δ 7.60-7.58 (m, 2H), 7.47-7.45 (m, 3H), 3.56 (s, 3H), 3.26 (t, *J* = 7.2 Hz, 2H), 2.51 (t, *J* = 7.3 Hz, 2H), 2.44 (bs, 4H), 2.04-1.98 (m, 2H), 1.61-1.57 (quint, *J* = 5.6 Hz, 4H), 1.41 (bs, 2H); ^{13}C NMR (125 MHz, $CDCl_3$) δ 155.9, 151.8, 130.0, 128.9, 128.6, 127.1, 57.5, 54.5, 31.6, 31.5, 26.5, 25.5, 24.1; LC-MS (ESI) m/z: 317.15 [M+H]

4,4-Dimethyl-1-(3-((4-methyl-5-phenyl-4H-1,2,4-triazol-3-yl)thio)propyl)piperidine (6d). A mixture of **6b**[14] (1.0 mmol), 4,4-dimethylpiperdine (1.1 mmol), and Cs_2CO_3 (1.5 mmol) was stirred in acetonitrile (3 mL) at 70 °C for 8 h. The crude reaction mixture was then filtered, and solvent was removed under reduced pressure. The residue was purified by flash chromatography on silica gel eluting with 10% 7 N NH_3 in MeOH solution/CH_2Cl_2 (1:10) affording **6d** as a white solid. (Yield 26%).^{1}H NMR (500 MHz, $CDCl_3$) δ 7.59-7.58 (m, 2H), 7.46-7.44 (m, 3H), 3.57 (s, 3H), 3.25 (t, *J* = 6.7 Hz, 2H), 2.92-2.89 (m, 2H), 2.80 (bs, 4H), 2.24-2.20 (m, 2H), 1.60 (bs, 4H), 0.93 (s, 6H); ^{13}C NMR (125 MHz, $CDCl_3$) δ 156.1, 151.3, 130.1, 128.9, 128.6, 126.9, 56.1, 49.6, 36.4, 31.7, 30.6, 28.0, 25.2; LC-MS (ESI) m/z: 345.18 [M+H]

Tert-butyl 9-(3-((4-methyl-5-phenyl-4H-1,2,4-triazol-3-yl)thio)propyl)-3,9-diazaspiro[5.5]undecane-3-carboxylate (6e). A mixture of **6b**[14] (1.0 mmol), tert-butyl 3,9-diazaspiro[5.5]undecane-3-carboxylate (1.1 mmol), and Cs_2CO_3 (1.5 mmol) was stirred in acetonitrile (5 mL) at 70 °C for 12 h. The crude reaction mixture was then filtered, and solvent was removed under reduced pressure. The residue was purified by flash chromatography on silica gel eluting with 10% 7 N NH_3 in MeOH solution/CH_2Cl_2 (1:10) affording **6e** as an off-white solid (Yield 47%). ^{1}H NMR (500 MHz, $CDCl_3$) δ 7.55-7.54 (m, 2H), 7.42-7.40 (m, 3H), 3.52 (s, 3H), 3.28-3.26 (m, 4H), 3.21 (t, *J* = 7.0 Hz, 2H), 2.51 (t, *J* = 7.1 Hz, 2H), 2.42 (bs, 4H), 1.99-1.93 (quint, *J* = 7.1 Hz, 2H), 1.48 (t, *J* = 5.6 Hz, 4H), 1.36 (s, 9H), 1.34 (bs, 4H); ^{13}C NMR (125 MHz, $CDCl_3$) δ 155.7, 154.8, 151.7, 129.9, 128.8, 128.4,

126.9, 79.1, 65.7, 56.9, 48.9, 39.6, 38.8, 34.8, 31.5, 30.9, 29.4, 28.3, 26.4, 15.2; LC-MS (ESI) m/z: 486.17 [M+H]

3-(2-((4-Methyl-5-phenyl-4H-1,2,4-triazol-3-yl)thio)propyl)-3,9-diazaspiro[5.5]undecane (6f). Compound was dissolved in CH_2Cl_2 (2 mL), followed by dropwise addition of CF_3COOH (2 mL), and stirred at room temperature for 3 h. Volatiles were then removed under reduced pressure, and the crude product was neutralized with a saturated $NaHCO_{3\ (aq)}$ solution (10 mL). The reaction mixture was extracted with CH_2Cl_2 (3 × 20 mL), and the organic layers were combined, dried, and concentrated to afford **6f** as an off-white solid (Yield 97%). (HCl salt) ^{1}H NMR (500 MHz, $(CD_3)_2SO$) δ 10.97 (bs, 1H), 7.78-7.76 (m, 2H), 7.62-7.59 (m, 3H), 3.65 (s, 3H), 3.35 (t, *J* = 6.9 Hz, 2H), 3.29-3.26 (m, 2H), 3.21-3.16 (m, 2H), 2.99 (bs, 6H), 2.22-2.17 (m, 2H), 1.83-1.77 (m, 6H), 1.54-1.52 (m, 2H); ^{13}C NMR (125 MHz, $(CD_3)_2SO$) δ 154.7, 151.2, 130.8, 128.9, 128.8, 125.0, 53.7, 47.0, 38.7, 38.6, 34.6, 32.2, 31.1, 30.1, 27.9, 26.7, 23.4; LC-MS (ESI) m/z: 386.68 [M+H]

1-(3-((4-Methyl-5-phenyl-4H-1,2,4-triazol-3-yl)thio)propyl)piperazine (6h). Following the procedure for **6f**, compound **6h** was obtained as a light tan oil. (Yield 12%). ^{1}H NMR (500 MHz, $CDCl_3$) δ 7.56-7.54 (m, 2H), 7.43-7.41 (m, 3H), 3.52 (s, 3H), 3.25-3.22 (m, 2H), 3.21 (s, 1H), 2.85-2.83 (t, *J* = 4.8 Hz, 4H), 2.42-2.38 (m, 6H), 1.95-1.89 (quint, *J* = 7.1 Hz, 2H); ^{13}C NMR (125 MHz, $CDCl_3$) δ 155.7, 151.9, 130.0, 128.8, 128.5, 127.0, 57.2, 53.8, 45.6, 31.5, 31.0, 26.5; LC-MS (ESI) m/z: 318.66 [M+H]

4-(5-((3-(9-(2-Methoxyphenyl)-3,9-diazaspiro[5.5]undecan-3-yl)propyl)thio)-4-methyl-4H-1,2,4-triazol-3-yl)-N,N-dimethylaniline (7). Following general method B, **7** was obtained as a tan oil. (Yield 48%). ^{1}H NMR (500 MHz, $CDCl_3$) δ 7.46 (d, *J* = 8.8 Hz, 2H), 6.92-6.89 (m, 2H), 6.86-6.83 (m, 1H), 6.80-6.78 (m, 1H), 6.72 (d, *J* = 8.8 Hz, 2H), 3.79 (s, 3H), 3.54 (s, 3H), 3.20 (t, *J* = 7.1 Hz, 2H), 2.96 (s, 3H), 2.93-2.91 (m, 4H), 2.65 (t, *J* = 7.1 Hz, 2H), 2.57 (bs, 4H), 2.08-2.02 (quint, *J* = 7.1 Hz, 2H), 1.63 (bs, 8H); ^{13}C NMR (125 MHz, $CDCl_3$) δ 156.4, 152.1, 151.1, 150.5, 141.9, 129.3, 122.6, 120.7, 118.1, 113.9, 111.7, 110.9, 56.7, 55.2, 48.9, 46.5, 45.8, 40.1, 35.8, 34.7, 31.6, 31.0, 28.9, 26.1; LC-MS (ESI) m/z: 535.32 [M+H]

3-(2-Methoxyphenyl)-9-(3-((5-(2-methoxyphenyl)-4-methyl-4H-1,2,4-triazol-3-yl)thio)propyl)-3,9-diazaspiro[5.5]undecane (8). Following general method B, **8** was obtained as a clear oil. (Yield 39%). ^{1}H NMR (500 MHz, $CDCl_3$) δ 7.46-7.43 (m, 2H), 7.05-7.02 (m, 1H), 6.97-6.95 (m, 1H), 6.93-6.92 (m, 2H), 6.88-6.86 (m, 1H), 6.81 (d, *J* = 7.8 Hz, 1H), 3.82 (s, 3H), 3.78 (s, 3H), 3.35 (s, 3H), 3.28 (t, *J* = 6.9 Hz, 2H), 2.94 (t, *J* = 4.6 Hz, 4H), 2.54 (t, *J* = 7.1 Hz, 2H), 2.47 (bs, 4H), 2.03-2.00 (m, 2H), 1.66-164 (m, 4H), 1.60-1.58 (m, 4H); ^{13}C NMR (125 MHz, $CDCl_3$) δ 157.2, 154.3, 152.2, 151.1, 142.1, 132.2, 132.0, 122.6, 121.0, 120.8, 118.2, 116.3, 111.0 (2xCH), 57.2, 55.5, 55.3, 49.2, 46.6, 36.0, 35.5, 31.1, 30.9, 29.1, 26.7; LC-MS (ESI) m/z: 522.23 [M+H]

3-(2-Methoxyphenyl)-9-(3-((4-methyl-5-(pyridin-3-yl)-4H-1,2,4-triazol-3-yl)thio)propyl)-3,9-diazaspiro[5.5]undecane (9). Following general method B, **9** was obtained as a light tan oil. (Yield 53%). ^{1}H NMR (500 MHz, $CDCl_3$) δ 8.85 (s, 1H), 8.69-8.68 (m, 1H), 7.98-7.96 (m, 1H), 7.43-7.40 (m, 1H), 6.94-6.90 (m, 2H), 6.86-6.83 (m, 1H), 6.80 (d, *J* = 7.7 Hz, 1H), 3.80 (s, 3H), 3.59 (s, 3H), 3.29 (t, *J* = 6.9 Hz, 2H), 2.94-2.92 (m, 4H), 2.56 (t, *J* = 6.3 Hz, 2H), 2.49 (bs, 4H), 2.06-2.00 (quint, *J* = 6.9 Hz, 2H), 1.64-1.62 (m, 4H), 1.60-1.58 (m, 4H); ^{13}C NMR (125 MHz, $CDCl_3$) δ 153.1, 152.7, 152.2, 151.0, 148.8, 142.0, 136.0, 123.7, 123.5, 122.6, 120.8, 118.1, 110.9, 57.0, 55.3, 49.2, 46.6, 36.0, 35.3, 31.6, 31.1, 29.0, 26.5, 22.6; LC-MS (ESI) m/z: 493.24 [M+H]

3-(2-Methoxyphenyl)-9-(3-((4-methyl-5-(4-(thiophen-3-yl)phenyl)-4H-1,2,4-triazol-3-yl)thio)propyl)-3,9-diazaspiro[5.5]undecane (10). Following general method B, **10** was obtained as a white solid. (Yield 15%) ^{1}H NMR (500 MHz, $CDCl_3$) δ 7.70 (d, *J* = 8.3 Hz, 2H), 7.65 (d, *J* = 8.3 Hz, 2H), 7.51-7.50 (m, 1H), 7.40-7.39 (m, 2H), 6.96-6.93 (m, 2H), 6.89-6.87 (m, 1H), 6.82 (d, *J* = 8.0 Hz, 1H), 3.82 (s, 3H), 3.59 (s, 3H), 3.29 (t, *J* = 7.2 Hz, 2H), 2.96-2.94 (m, 4H), 2.49 (t, *J* = 7.5 Hz, 2H), 2.42-2.40 (m, 4H), 2.02-1.96 (quint, *J* = 7.1 Hz, 2H), 1.66-1.64 (m, 4H), 1.57-1.55 (m, 4H); ^{13}C NMR (125 MHz, $CDCl_3$) δ 155.5, 152.2, 152.0, 142.1, 141.1, 137.2, 128.9, 126.7, 126.6, 126.0, 125.6, 122.5, 121.3, 120.8, 118.1, 110.9, 57.3, 55.3, 49.2, 46.6, 36.1, 35.8, 31.6, 31.3, 29.1, 26.9; LC-MS (ESI) m/z: 574.19 [M+H]

2-(4-(5-((3-(9-(2-Methoxyphenyl)-3,9-diazaspiro[5.5]undecan-3-yl)propyl)thio)-4-methyl-4H-1,2,4-triazol-3-yl)phenyl)oxazole (11). Following general method B, **11** was obtained as a beige solid. (Yield 17%) ^{1}H NMR (500 MHz, $CDCl_3$) δ 8.17 (d, J = 8.2 Hz, 2H), 7.75 (s, 1H), 7.74 (s, 2H), 7.26 (s, 1H), 6.94-6.93 (m, 2H), 6.89-6.87 (m, 1H), 6.83 (d, J = 7.8 Hz, 1H), 3.83 (s, 3H), 3.62 (s, 3H), 3.32-3.29 (t, J = 7.0 Hz, 2H), 2.96-2.94 (m, 2H), 2.56-2.53 (m, 2H), 2.47 (bs, 4h), 2.06-2.00 (quint, J = 7.0 Hz, 2H), 1.66-1.64 (m, 4H), 1.60-1.58 (m, 4H); ^{13}C NMR (125 MHz, $CDCl_3$) δ 161.0, 155.1, 152.4, 152.3, 142.2, 139.2, 128.9, 128.8, 128.7, 126.8, 122.6, 120.9, 118.2, 111.0, 57.2, 55.3, 49.5, 49.3, 46.7, 36.1, 35.5, 31.8, 31.2, 29.1, 26.8; LC-MS (ESI) m/z: 559.23 [M+H]

3-(3-((5-(2-Fluorophenyl)-4-methyl-4H-1,2,4-triazol-3-yl)thio)propyl)-9-(2-methoxyphenyl)-3,9-diazaspiro[5.5]undecane (12). Following general method B, **12** was obtained as a beige solid. (Yield 44%) ^{1}H NMR (500 MHz, $CDCl_3$) δ 7.56-7.53 (m, 1H), 7.46-7.44 (m, 1H), 7.25-7.21 (m, 1H), 7.16-7.12 (m, 1H), 6.91-6.88 (m, 1H), 6.86-6.81 6.83 (m, 2H), 6.79-6.76 (m, 1H), 3.77 (s, 3H), 3.41 (s, 3H), 3.29-3.26 (t, J = 6.7 Hz, 2H), 2.99 (bs, 2H), 2.90 (bs, 8H), 2.28 (m, 2h), 1.81 (bs, 4H), 1.65 (m, 4H); ^{13}C NMR (125 MHz, $CDCl_3$) δ 158.7 (d, $J_{C–F}$ = 250.3 Hz), 152.2, 152.1, 151.5, 141.7, 132.7 (d, $J_{C–C–C–F}$ = 8.1 Hz), 132.1, 124.9 (d, $J_{C–C–C–F}$ = 3.0 Hz), 122.8, 120.8, 118.2, 116.1 (d, $J_{C–C–F}$ = 21.1 Hz), 115.1 (d, $J_{C–C–F}$ = 14.3 Hz), 111.0, 55.8, 55.3, 48.7, 46.5, 35.5 (bs), 33.2, 31.2 (d, $J_{CH3–F}$ = 5.7 Hz), 30.4, 28.7, 24.8; LC-MS (ESI) m/z: 510.78 [M+H]

3-(3-((5-(4-Fluorophenyl)-4-methyl-4H-1,2,4-triazol-3-yl)thio)propyl)-9-(2-methoxyphenyl)-3,9-diazaspiro[5.5]undecane (13). Following general method B, **13** was obtained as a white solid. (Yield 24%) ^{1}H NMR (500 MHz, $CDCl_3$) δ 7.63-7.60 (m, 2H), 7.19-7.15 (m, 2H), 6.97-6.93 (m, 1H), 6.91-6.85 (m, 2H), 6.82-6.80 (m, 1H), 3.82 (s, 3H), 3.59 (s, 3H), 3.30-3.28 (t, J = 6.9 Hz, 2H), 3.06-3.03 (m, 2H), 3.00 (bs, 2H), 2.95-2.93 (m, 6h), 2.36-2.32 (quint, J = 6.8 Hz, 2H), 1.88 (bs, 4H), 1.70 (bs, 4H); ^{13}C NMR (125 MHz, $CDCl_3$) δ 162.8 (d, $J_{C–F}$ = 250.7 Hz), 155.3, 152.2, 151.2, 141.6, 130.7 (d, $J_{C–C–C–F}$ = 8.4 Hz), 123.1 (d, $J_{C–C–C–F}$ = 3.8 Hz), 122.9, 120.9, 118.2, 116.3 (d, $J_{C–C–F}$ = 22.0 Hz), 111.1, 55.8, 55.4, 48.7, 46.5, 33.2 (bs), 31.8, 30.4, 28.7, 24.7; LC-MS (ESI) m/z: 510.63 [M+H]

3-(3-((5-Cyclohexyl-4-methyl-4H-1,2,4-triazol-3-yl)thio)propyl)-9-(2-methoxyphenyl)-3,9-diazaspiro[5.5]undecane (14). Following general method B, **14** was obtained as a white semi-solid. (Yield 39%) ^{1}H NMR (500 MHz, $CDCl_3$) δ 6.95-6.91 (m, 2H), 6.87-6.84 (m, 1H), 6.81-6.79 (m, 1H), 3.81 (s, 3H), 3.44 (s, 3H), 3.15 (t, *J* = 7.0 Hz, 2H), 2.94-2.92 (m, 4H), 2.60-2.54 (m, 3H), 2.50 (bs, 4H), 2.01-1.96 (quint, *J* = 7.0 Hz, 2H), 1.90-1.82 (m, 4H), 1.71-1.67 (m, 2H), 1.65-1.59 (m, 9H), 1.36-1.26 (m, 3H); ^{13}C NMR (125 MHz, $CDCl_3$) δ 159.5, 152.2 149.9, 142.0, 122.6, 120.8, 118.1, 110.9, 57.0, 55.3, 49.1, 46.6, 35.9, 35.0, 31.2, 30.7, 29.8, 29.0, 26.4, 26.0, 25.6; LC-MS (ESI) m/z: 498.32 [M+H]

3-(3-((4-Ethyl-5-phenyl-4H-1,2,4-triazol-3-yl)thio)propyl)-9-(2-methoxyphenyl)-3,9-diazaspiro[5.5]undecane (15). Following general method B, **15** was obtained as a white solid. (Yield 55%) ^{1}H NMR (500 MHz, $CDCl_3$) δ 7.56-7.54 (m, 2H), 7.46-7.44 (m, 3H), 6.93-6.89 (m, 2H), 6.87-6.85 (m, 1H), 6.81-6.79 (m, 1H), 3.96-3.92 (quart, *J* = 7.2 Hz, 2H), 3.80 (s, 3H), 3.30 (t, *J* = 7.1 Hz, 2H), 2.94-2.92 (m, 4H), 2.76 (t, *J* = 7.0 Hz, 2H), 2.69 (bs, 4H), 2.20-2.14 (quint, *J* = 7.1 Hz, 2H), 1.71-1.69 (m, 4H), 1.67-1.65 (m, 4H), 1.27 (t, *J* = 7.2 Hz, 3H); ^{13}C NMR (125 MHz, $CDCl_3$) δ 155.5, 152.1, 150.9, 141.8, 130.0, 128.9, 128.5, 127.2, 122.7, 120.8, 118.1, 111.0, 56.6, 55.3, 48.9, 46.5, 39.6, 35.6, 34.3, 30.8, 28.9, 25.8, 15.4; LC-MS (ESI) m/z: 506.20 [M+H]

3-((3-(9-(2-Methoxyphenyl)-3,9-diazaspiro[5.5]undecan-3-yl)propyl)thio)-5-phenyl-4H-1,2,4-triazol-4-amine (16). Following general method B, **16** was obtained as a clear oil. (Yield 46%) ^{1}H NMR (500 MHz, $CDCl_3$) δ 8.03-8.01 (m, 2H), 7.42-7.41 (m, 3H), 6.97-6.91 (m, 2H), 6.89-6.88 (m, 1H), 6.82 (d, *J* = 8.0 Hz, 1H), 5.18 (s, 2H), 3.82 (s, 3H), 3.18 (t, *J* = 6.9 Hz, 2H), 2.94-2.92 (m, 4H), 2.53 (t, *J* = 7.0 Hz, 2H), 2.47-2.45 (m, 4H), 1.97-1.91 (quint, *J* = 7.2 Hz, 2H), 1.64-162 (m, 4H), 1.58-1.56 (m, 4H); ^{13}C NMR (125 MHz, $CDCl_3$) δ 154.3, 152.8, 152.2, 142.0, 130.0, 128.5, 128.2, 126.5, 122.7, 120.9, 118.2, 111.0, 56.8, 55.3, 49.1, 46.6, 35.9, 35.2, 30.9, 29.0, 26.5; LC-MS (ESI) m/z: 493.24 [M+H]

3-(2-Methoxyphenyl)-9-(3-((5-phenyl-4H-1,2,4-triazol-3-yl)thio)propyl)-3,9-diazaspiro[5.5]undecane (17). Following general method B, **17** was obtained as a clear oil. (Yield 41%) ^{1}H NMR (500 MHz, $CDCl_3$) δ 11.1 (bs, 1H), 8.04 (d, *J* = 7.6 Hz, 2H), 7.36-7.30 (m, 3H), 6.96-6.92 (m,

2H), 6.89-6.86 (m, 1H), 6.81 (d, *J* = 8.0 Hz, 1H), 3.79 (s, 3H), 3.10 (t, *J* = 6.4 Hz, 2H), 2.96-2.94 (m, 4H), 2.57 (t, *J* = 6.3 Hz, 2H), 2.49 (bs, 4H), 1.98-1.92 (quint, *J* = 6.2 Hz, 2H), 1.69-1.66 (m, 8H); ^{13}C NMR (125 MHz, $CDCl_3$) δ 161.1, 155.7, 152.0, 141.8, 130.0, 129.0, 128.3, 126.2, 122.6, 120.7, 118.1, 110.9, 55.1, 54.8, 48.8, 46.5, 35.6, 34.7, 30.3.28.9, 26.5; LC-MS (ESI) m/z: 478.15 [M+H]

3-(2-Methoxyphenyl)-9-(3-((5-phenyl-1H-imidazol-2-yl)thio)propyl)-3,9-diazaspiro[5.5]undecane (18). Following general method B, **18** was obtained as a light grey solid. (Yield 82%) ^{1}H NMR (500 MHz, $CDCl_3$) δ 10.92 (bs, 1H), 7.73 (d, *J* = 7.1 Hz, 2H), 7.31 (t, *J* = 7.7 Hz, 2H), 7.28 (s, 3H), 7.18 (t, *J* = 7.3 Hz, 1H), 6.99-6.88 (m, 3H), 6.84-6.83 (d, *J* = 7.8 Hz, 1H), 3.83 (s, 3H), 3.01 (t, *J* = 6.0 Hz, 2H), 2.97-2.95 (m, 4H), 2.67 (t, *J* = 6.6 Hz, 2H), 2.55 (bs, 4H), 1.93-1.88 (quint, *J* = 6.4 Hz, 2H), 1.68-1.64 (m, 8H); ^{13}C NMR (125 MHz, $CDCl_3$) δ 152.2, 141.9, 141.8, 141.0, 133.4, 128.5, 126.6, 124.7, 122.7, 120.8, 118.2, 115.7, 111.1, 55.3, 54.8, 48.5, 46.5, 35.6, 35.0, 32.0, 29.0, 26.2; LC-MS (ESI) m/z: 477.22 [M+H]

3-(2-Methoxyphenyl)-9-(3-((1-methyl-5-phenyl-1H-imidazol-2-yl)thio)propyl)-3,9-diazaspiro[5.5]undecane (19). Following general method B, **19** was obtained as a tan oil. (Yield 35%) ^{1}H NMR (500 MHz, $CDCl_3$) δ 7.39-7.36 (m, 2H), 7.32-7.31 (m, 3H), 7.05 (s, 1H), 6.92-6.90 (m, 2H), 6.86-6.85 (m, 1H), 6.80-6.79 (m, 1H), 3.80 (s, 3H), 3.54 (s, 3H), 3.12-3.10 (t, *J* = 6.9 Hz, 2H), 2.94-2.92 (m, 4H), 2.59-2.56 (t, *J* = 6.5 Hz, 2H), 2.51 (bs, 4H), 1.98-1.95 (m, 2H), 1.65-1.60 (m, 8H); ^{13}C NMR (125 MHz, $CDCl_3$) δ 152.1, 142.7, 142.0, 129.9, 128.6, 128.3, 127.8, 122.5, 120.8, 118.1, 111.0, 57.0, 55.2, 49.0, 46.5, 35.8 (bs), 35.0, 32.0, 28.9, 26.5; LC-MS (ESI) m/z: 491.73 [M+H]

3-(2-Methoxyphenyl)-9-(2-((4-methyl-5-phenyl-4H-1,2,4-triazol-3-yl)thio)ethyl)-3,9-diazaspiro[5.5]undecane (20). Following general method B, **20** was obtained as a tan oil. (Yield 12%) ^{1}H NMR (500 MHz, $CDCl_3$) δ 7.62-7.60 (m, 2H), 7.48-7.46 (m, 3H), 6.96-6.93 (m, 2H), 6.89-6.86 (m, 1H), 6.83-6.81 (m, 1H), 3.83 (s, 3H), 3.58 (s, 3H), 3.44 (t, *J* = 6.7 Hz, 2H), 2.96-2.94 (m, 4H), 2.81 (t, *J* = 6.7 Hz, 2H), 2.52-2.49 (m, 4H), 1.65-1.63 (m, 4H), 1.57-1.55 (m, 4H); ^{13}C NMR (125 MHz, $CDCl_3$) δ 155.8, 152.2, 152.1, 142.1, 130.0, 128.9, 128.5, 127.1, 122.6, 120.8, 118.2, 111.0, 57.8, 55.3, 49.0, 46.7, 36.0, 35.5, 31.7, 30.6, 29.1; LC-MS (ESI) m/z: 478.42 [M+H]

3-(2-Methoxyphenyl)-9-(4-((4-methyl-5-phenyl-4H-1,2,4-triazol-3-yl)thio)butyl)-3,9-diazaspiro[5.5]undecane (21). Following general method B, **21** was obtained as a tan oil. (Yield 14%) ^{1}H NMR (500 MHz, $CDCl_3$) δ 7.61-7.59 (m, 2H), 7.48-7.46 (m, 3H), 6.96-6.91 (m, 2H), 6.88-6.87 (m, 1H), 6.82-6.81 (m, 1H), 3.82 (s, 3H), 3.58 (s, 3H), 3.27 (t, J = 6.9 Hz, 2H), 2.96-2.94 (m, 4H), 2.61-2.50 (m, 6H), 1.84-1.78 (m, 4H), 1.67-1.66 (m, 8H); ^{13}C NMR (125 MHz, $CDCl_3$) δ 155.9, 152.3, 151.9, 142.0, 130.1, 128.9, 128.6, 127.1, 122.7, 120.9, 118.2, 111.1, 57.9, 55.3, 49.1, 46.6, 34.8, 32.8, 31.6, 29.0, 27.5, 25.1, 22.6; LC-MS (ESI) m/z: 506.20 [M+H]

3-(2-Ethoxyphenyl)-9-(3-((4-methyl-5-phenyl-4H-1,2,4-triazol-3-yl)thio)propyl)-3,9-diazaspiro[5.5]undecane (22). Following general method B, **22** was obtained as a dark tan oil. (Yield 13%) ^{1}H NMR (500 MHz, $CDCl_3$) δ 7.60-7.58 (m, 2H), 7.47-7.45 (m, 3H), 6.90-6.88 (m, 2H), 6.87-6.85 (m, 1H), 6.84-6.78 (m, 1H), 4.03-3.99 (m, 2H), 3.55 (s, 3H), 3.28 (t, J = 7.1 Hz, 2H), 2.98-2.96 (m, 4H), 2.50 (t, J = 7.3 Hz, 2H), 2.43 (bs, 4H), 2.02-1.97 (quint, J = 7.0 Hz, 2H), 1.64-1.62 (m, 4H), 1.57-1.56 (m, 4H), 1.41 (t, J = 7.0 Hz, 3H); ^{13}C NMR (125 MHz, $CDCl_3$) δ 155.7, 151.8, 151.5, 142.2, 129.9, 128.8, 128.5, 127.1, 122.3, 120.8, 118.1, 112.3, 63.4, 57.2, 49.2, 46.5, 36.1, 35.7, 31.5, 31.2, 29.1, 26.8, 14.9; LC-MS (ESI) m/z: 506.20 [M+H]

2-(9-(3-((4-Methyl-5-phenyl-4H-1,2,4-triazol-3-yl)thio)propyl)-3,9-diazaspiro[5.5]undecan-3-yl)phenol (23). Following general method B, **23** was obtained as a dark tan oil. (Yield 13%) ^{1}H NMR (500 MHz, $CDCl_3$) δ 7.63-7.60 (m, 2H), 7.50-7.48 (m, 3H), 7.15-7.13 (dd, J_1 = 1.4 Hz, J_2 = 1.4 Hz, 1H), 7.05-7.02 (dt, J_1 = 1.4 Hz, J_2 = 7.9 Hz, 1H), 6.93-6.91 (dd, J_1 = 1.4 Hz, J_2 = 8.0 Hz, 1H), 6.84-6.81 (dt, J_1 = 1.4 Hz, J_2 = 7.6 Hz, 1H), 3.59 (s, 3H), 3.32-3.29 (t, J = 7.0 Hz, 2H), 2.79-2.77 (m, 4H), 2.58-2.55 (t, J = 7.3 Hz, 2H), 2.50 (bs, 4H), 2.07-2.01 (m, 2H), 1.99 (s, 1H), 1.64-1.62 (m, 8H); ^{13}C NMR (125 MHz, $CDCl_3$) δ 155.9, 151.9, 151.5, 139.9, 130.1, 129.0, 128.6, 127.2, 126.2, 121.2, 119.9, 113.9, 57.2, 49.2, 48.7, 36.7, 35.6, 31.7, 31.2, 29.1, 26.8, 22.7; LC-MS (ESI) m/z: 478.66 [M+H]

3-(2-(2-Fluoroethoxy)phenyl)-9-(3-((4-methyl-5-phenyl-4H-1,2,4-triazol-3-yl)thio)propyl)-3,9-diazaspiro[5.5]undecane (24). Following general method B, **24** was obtained as a white solid. (Yield

12%) ^{1}H NMR (500 MHz, $CDCl_3$) δ 7.61-7.59 (m, 2H), 7.47-7.45 (m, 3H), 6.92-6.89 (m, 3H), 6.81-6.79 (m, 1H), 4.78-4.77 (m, 1H), 4.69-4.67 (m, 1H), 4.24-4.22 (m, 1H), 4.18-4.16 (m, 1H), 3.57 (s, 3H), 3.27 (t, J = 7.0 Hz, 2H), 2.98-2.96 (m, 4H), 2.85-2.82 (m, 2H), 2.76 (bs, 4H), 2.21-2.16 (quint, J = 7.2 Hz, 2H), 1.75-1.73 (m, 4H), 1.66-164 (m, 4H); ^{13}C NMR (125 MHz, $CDCl_3$) δ 156.0, 151.4, 150.9, 142.4, 130.1, 128.9, 128.5, 126.9, 122.5, 122.0, 118.5, 113.4, 82.7 (d, $J_{C–F}$ = 170.1 Hz, CH_2F), 67.5 (d, $J_{C–F}$ = 20.1 Hz, O–CH_2CH_2F), 56.4, 48.9, 46.4, 35.6, 34.0, 31.7, 30.7, 28.9, 25.5; LC-MS (ESI) m/z: 524.23 [M+H]

3-(2,4-Dimethoxyphenyl)-9-(3-((4-methyl-5-phenyl-4H-1,2,4-triazol-3-yl)thio)propyl)-3,9-diazaspiro[5.5]undecane (26). Following general method B, **26** was obtained as an off-white solid. (Yield 8%) ^{1}H NMR (500 MHz, $CDCl_3$) δ 7.62-7.60 (m, 2H), 7.49-7.47 (m, 3H), 6.85-6.83 (m, 1H), 6.44-6.43 (m, 1H), 6.39-6.37 (m, 1H), 3.80 (s, 3H), 3.74 (s, 3H), 3.28 (t, J = 6.9 Hz, 2H), 2.88-2.87 (m, 4H), 2.75 (t, J = 7.0 Hz, 2H), 2.67 (bs, 4H), 2.17-2.11 (quint, J = 7.0 Hz, 2H), 1.69-1.66 (m, 8H); ^{13}C NMR (125 MHz, $CDCl_3$) δ 156.0, 153.4, 151.6, 135.9, 130.1, 128.9, 128.6, 127.0, 118.5, 103.3, 99.8, 56.7, 55.5, 55.4, 49.1, 47.2, 36.0, 34.6, 31.7, 30.9, 28.9, 26.0; LC-MS (ESI) m/z: 522.09 [M+H]

3-(2-Fluorophenyl)-9-(3-((4-methyl-5-phenyl-4H-1,2,4-triazol-3-yl)thio)propyl)-3,9-diazaspiro[5.5]undecane (28). Following general method B, **28** was obtained as an off-white solid. (Yield 13%) ^{1}H NMR (500 MHz, $CDCl_3$) δ 7.62-7.60 (m, 2H), 7.49-7.46 (m, 3H), 7.02-6.95 (m, 1H), 6.94-6.90 (m, 1H), 6.89-6.87 (m, 1H), 3.58 (s, 3H), 3.29-3.27 (t, J = 7.0 Hz, 2H), 2.99-2.97 (m, 4H), 2.74 (bs, 2H), 2.67 (bs, 4H), 2.15-2.12 (m, 2H), 1.68-1.64 (m, 8H); ^{13}C NMR (125 MHz, $CDCl_3$) δ 156.0, 154.8 (d, $J_{C–F}$ = 245.4 Hz), 151.6, 140.7 (d, $J_{C–C–F}$ = 8.3 Hz), 130.1, 128.9, 128.6, 127.1, 127.1, 124.4 (d, $J_{C–C–C–F}$ = 3.5 Hz), 122.2 (d, $J_{C–C–C–F}$ = 7.8 Hz), 119.1 (d, $J_{C–C–C–C–F}$ = 2.7 Hz), 116.1 (d, $J_{C–C–F}$ = 20.9 Hz), 56.7, 49.0, 46.0 (2XCH), 35.6 (bs), 34.5, 31.7, 30.9, 28.9, 26.0; LC-MS (ESI) m/z: 480.16 [M+H]

3-(2-Fluoro-4-(trifluoromethyl)phenyl)-9-(3-((4-methyl-5-phenyl-4H-1,2,4-triazol-3-yl)thio)propyl)-3,9-diazaspiro[5.5]undecane (29). Following general method B, **29** was obtained as a white solid. (Yield 28%) ^{1}H NMR (500 MHz, $CDCl_3$) δ 7.62-7.60 (m, 2H), 7.49-7.46 (m, 3H), 7.28-7.26 (m, 1H), 7.22-7.19 (dd, J_1 = 1.8 Hz, J_2 = 12.7 Hz, 1H), 6.96-6.92 (t, J = 8.3 Hz, 1H), 3.58 (s, 3H), 3.30-

3.27 (t, J = 7.0 Hz, 2H), 3.08-3.05 (m, 4H), 2.75 (bs, 2H), 2.67 (bs, 4H), 2.15-2.12 (m, 2H), 1.79-1.68 (m, 4H), 1.66-1.64 (m, 4H); ^{13}C NMR (125 MHz, $CDCl_3$) δ 156.0, 153.6 (d, $J_{C–F}$ = 249.6 Hz), 151.6, 143.5 (d, $J_{C–C–C–F}$ = 8.5 Hz), 130.1, 129.0, 128.6, 127.1, 121.7 (q, $J_{C–C–CF3}$ = 3.5 Hz), 118.7 (d, $J_{C–C–C–F}$ = 3.6 Hz), 113.4 (d, $J_{C–C–F}$ = 21.0 Hz) and (quint, $J_{C–C–C–CF3}$ = 3.4 Hz), 56.7, 49.0, 46.0 (2XCH), 35.4 (bs), 34.5, 31.7, 30.9, 29.0, 26.1; LC-MS (ESI) m/z: 548.14 [M+H]

3-(4-Fluoro-2-methoxyphenyl)-9-(3-((4-methyl-5-phenyl-4H-1,2,4-triazol-3-yl)thio)propyl)-3,9-diazaspiro[5.5]undecane (30). Following general method B, **30** was obtained as an off-white solid. (Yield 24%) ^{1}H NMR (500 MHz, $CDCl_3$) δ 7.59-7.57 (m, 2H), 7.45-7.43 (m, 3H), 6.83-6.80 (m, 1H), 6.54-6.51 (m, 2H), 6.89-6.87, 3.78 (s, 3H), 3.54 (s, 3H), 3.28-3.25 (t, J = 7.1 Hz, 2H), 2.86-2.85 (m, 4H), 2.47-2.44 (t, J = 7.1 Hz, 2H), 2.38 (bs, 4H), 1.97-1.95 (quint, J = 7.1 Hz, 2H), 1.62-1.60 (m, 4H), 1.54-1.51 (m, 4H); ^{13}C NMR (125 MHz, $CDCl_3$) δ 157.9 (d, $J_{C–F}$ = 239.7 Hz), 155.7, 153.2 (d, $J_{C–C–C–F}$ = 9.3 Hz), 151.9, 138.4 (d, $J_{C–C–C–C–F}$ = 2.7 Hz), 129.9, 128.8. 128.5, 127.1, 118.4 (d, $J_{C–C–C–F}$ = 9.6 Hz), 106.0 (d, $J_{C–C–F}$ = 20.9 Hz), 99.6 (d, $J_{C–C–F}$ = 26.5 Hz), 57.3, 55.6, 49.2, 47.0, 35.8 (bs), 31.5, 31.2, 29.0, 27.0; LC-MS (ESI) m/z: 510.63 [M+H]

3-(2-Methoxyphenyl)-9-(3-((4-methyl-5-phenyl-4H-1,2,4-triazol-3-yl)thio)propyl)-3,9-diazaspiro[5.5]undec-1-ene (32). Following general method B, **32** was obtained as a dark red oil. (Yield 18%) ^{1}H NMR (500 MHz, $CDCl_3$) δ 7.64-7.62 (m, 2H), 7.51-7.49 (m, 3H), 7.02-6.98 (m, 1H), 6.94-6.92 (m, 1H), 6.90-6.86 (m, 2H), 6.27-6.26 (d, J = 8.1 Hz, 1H), 4.62 (d, J = 7.9 Hz, 1H), 3.83 (s, 3H), 3.60 (s, 3H), 3.43-3.41 (m, 2H), 3.32 (t, J = 7.0 Hz, 2H), 2.80-2.74 (m, 4H), 2.73-2.67 (bs, 2H), 2.20-2.14 (quint, J = 7.5 Hz, 2H), 1.75-1.72 (m, 6H); ^{13}C NMR (125 MHz, $CDCl_3$) δ 156.1, 152.4, 151.7, 137.5, 132.2, 130.2, 129.0, 128.7, 127.1, 123.8, 122.3, 121.1, 112.0, 56.9, 55.7, 49.5, 44.3, 37.7, 31.7, 31.0, 29.7, 26.1; LC-MS (ESI) m/z: 490.17 [M+H]

8-(2-Methoxyphenyl)-2-(3-((4-methyl-5-phenyl-4H-1,2,4-triazol-3-yl)thio)propyl)-2,8-diazaspiro[4.5]decane (34). Following general method B, **34** was obtained as a tan semi-solid. (Yield 40%) ^{1}H NMR (500 MHz, $CDCl_3$) δ 7.58-7.57 (m, 2H), 7.45-7.43 (m, 3H), 6.94-6.91 (m, 1H), 6.86-6.83

(m, 2H), 6.79-6.76 (m, 1H), 3.18 (s, 3H), 3.57 (s, 3H), 3.29-3.26 (m, 2H), 3.21-3.10 (m, 4H), 3.00 (bs, 2H), 2.91 (bs, 4H), 2.30-2.27 (m, 2H), 1.93 (bs, 2H), 1.84 (bs, 4H); ^{13}C NMR (125 MHz, $CDCl_3$) δ 156.1, 152.1, 151.0, 141.4, 130.1, 128.9, 128.5, 126.8, 122.9, 120.8, 118.3, 111.0, 55.3, 54.4, 52.9, 48.4, 40.3, 36.7, 35.2, 31.7, 30.2, 26.2; LC-MS (ESI) m/z: 478.81 [M+H]

N-(4-(9-(2-Methoxyphenyl)-3,9-diazaspiro[5.5]undecan-3-yl)butyl)-4-(thiophen-3-yl)benzamide (35). Compound **F** (1.0 mmol), 4-(thiophen-3-yl)benzoic acid (1.1 mmol), 1-hydroxybenzotriazole (HOBt) hydrate (1.0 mmol), 1-ethyl-3-(3'-dimethylaminopropyl)carbodiimide (EDC) · HCl (1.0 mmol) were stirred in 15 mL of CH_2Cl_2 at room temperature for 2 h. The reaction mixture was then washed with a saturated $NaHCO_{3\,(aq)}$ solution (10 mL). The reaction mixture was extracted with CH_2Cl_2 (3 × 20 mL), and the organic layers were combined, dried, and concentrated to afford a crude white sold. Residue was purified by flash chromatography on silica gel eluting with MeOH/CH_2Cl_2 (1:10) to afford **35** as a white solid. (Yield 31%) ^{1}H NMR (500 MHz, $(CD_3)_2SO$) δ 8.66 (m, 1H), 8.00 (bs, 1H), 7.95 (d, *J* = 7.7 Hz, 2H), 7.82 (d, *J* = 8.2 Hz, 2H), 7.67-7.65 (m, 1H), 7.63-7.62 (m, 1H), 6.91-6.88 (m, 3H), 6.85-6.83 (m, 1H), 3.75 (s, 3H), 3.31 (quint, *J* = 5.9 Hz, 2H), 2.96-2.87 (m, 9H), 1.69 (bs, 6H), 1.57-1.56 (m, 6H); ^{13}C NMR (125 MHz, $(CD_3)_2SO$) δ 165.7, 152.0, 141.8, 140.5, 137.5, 132.8, 127.9, 127.3, 126.2, 125.7, 122.3, 122.2, 120.7, 118.1, 111.7, 55.2, 47.5, 45.8, 38.5, 32.6, 28.4, 26.5, 21.5; LC-MS (ESI) m/z: 518.22 [M+H]

4-(Dimethylamino)-N-(4-(9-(2-methoxyphenyl)-3,9-diazaspiro[5.5]undecan-3-yl)butyl)benzamide (36). Compound **F** (1.0 mmol), 4-dimethylamino benzoic acid (1.1 mmol), 1-hydroxybenzotriazole (HOBt) hydrate (1.0 mmol), 1-ethyl-3-(3'-dimethylaminopropyl)carbodiimide (EDC) · HCl (1.0 mmol) were stirred in 15 mL of CH_2Cl_2 at room temperature for 2 h. The reaction mixture was then washed with a saturated $NaHCO_{3\,(aq)}$ solution (10 mL). The reaction mixture was extracted with CH_2Cl_2 (3 × 20 mL), and the organic layers were combined, dried, and concentrated to afford a crude white sold. Residue was purified by flash chromatography on silica gel eluting with MeOH/CH_2Cl_2 (1:10) to afford **36** as a white solid. (Yield 40%) ^{1}H NMR (500 MHz, $CDCl_3$) δ 7.85 (d, *J* = 8.8 Hz, 2H), 7.33 (bs, 1H), 6.99-6.96 (m, 1H), 6.92-6.88 (m, 2H), 6.84-6.83 (m, 1H), 6.65 (d, *J* = 8.9 Hz, 2H), 3.84 (s, 3H), 3.47-3.44 (m, 2H),

3.10-2.95 (m, 16H), 1.91-1.90 (m, 6H), 1.71-1.67 (m, 6H); ^{13}C NMR (125 MHz, $CDCl_3$) δ 167.8, 152.4, 152.2, 141.5, 128.8, 123.1, 121.0, 120.9, 118.3, 111.2, 111.1, 56.3, 55.4, 48.4, 46.5, 40.2, 38.0, 32.4, 28.7,26.5, 21.1; LC-MS (ESI) m/z: 479.35 [M+H]

7-(3-(9-(2-Methoxyphenyl)-3,9-diazaspiro[5.5]undecan-3-yl)propoxy)-3,4-dihydroquinolin-2(1H)-one (37). 4b' (1.5 mmol), **G**[17] (1.5 mmol), KI (1.5 mmol) and K_2CO_3 (5.0 mmol) were dissolved in acetonitrile (15 mL), and the reaction mixture was stirred at 90 °C for 12 h. The reaction mixture was then filtered and solvent was removed under reduced pressure. Crude residue was purified by silica gel column chromatography eluting with 10% 7 N NH_3 in MeOH solution/CH_2Cl_2 (1:10) to afford **37** as a white solid (Yield 62%). ^{1}H NMR (500 MHz, $CDCl_3$) δ 8.88 (s, 1H), 7.02-7.00 (d, J = 8.4 Hz, 1H), 6.98-6.95 (m, 2H), 6.91-6.88 (m, 1H), 6.84-6.83 (d, J = 8.0 Hz, 1H), 6.52-6.50 (dd, J_1 = 2.1 Hz, J_2 = 8.2 Hz, 1H), 6.37-6.36 (m, 1H), 3.97-3.95 (t, J = 6.1 Hz, 2H), 3.84 (s, 3H), 2.99-2.97 (m, 4H), 2.89-2.86 (t, J = 7.4 Hz, 2H), 2.61-2.58 (t, J = 7.9 Hz, 2H), 2.53-2.50 (t, J = 7.0 Hz, 2H), 2.45 (bs, 4H), 2.01-1.95 (m, 2H), 1.69-1.67 (m, 4H), 1.61-1.59 (m, 4H); ^{13}C NMR (125 MHz, $CDCl_3$) δ 172.2, 158.7, 152.3, 142.3, 138.3 (2xCH), 128.6, 122.6, 120.9, 118.3, 115.7, 111.1, 108.7, 102.4, 66.7, 55.7, 55.4, 49.4, 46.8, 36.2 (bs), 35.8, 31.1, 29.2, 26.9, 24.6; LC-MS (ESI) m/z: 464.68 [M+H]

Receptor Binding Assays: Receptor K_i values were measured using human D_2 (long) and D_3 expressed in HEK cells with [^{125}I]IABN as the radioligand. The binding properties of membrane-associated receptors were characterized by a filtration binding assay.[37] Membrane homogenates were suspended in 50 mM Tris-HCl/150 mM NaCl/10 mM EDTA buffer, pH 7.5, and incubated with [^{125}I]IABN[37] at 37 °C for 60 min, using 20 μM (+)-butaclamol to define the nonspecific binding.

The radioligand concentration was equal to approximately 0.5 ($D_{2/3}R$) times the K_d, and the concentration of the competitive inhibitor ranged over 5 orders of magnitude. For each competition curve, two concentrations of inhibitor per decade were used, and triplicates were performed. Binding was terminated by the addition of ice cold wash buffer ($D_{2/3}R$, 10 mM Tris-HCl, 150 mM NaCl, pH 7.5; 5-$HT_{1A}R$, 10 mM Tris-HCl, pH 7.4) and filtration over a glass-fiber filter ($D_{3/2}R$, Schleicher and Schuell

No. 32; 5-HT_{1A}R, Whatman grade 934-AH, GE Healthcare Bio-Sciences, Pittsburgh, PA). A Packard Cobra scintillation counter was used to measure the radioactivity. The equilibrium dissociation constant and maximum number of binding sites were generated using unweighted nonlinear regression analysis of data modeled according to the equation describing mass R-binding. The concentration of inhibitor that inhibits 50% of the specific binding of the radioligand (IC_{50}) was determined by using nonlinear regression analysis to analyze the data of competitive inhibition experiments. Competition curves were modeled for a single site, and the IC_{50} values were converted to equilibrium dissociation constants (K_i) using the Cheng and Prusoff[51] correction. Mean K_i ± SEM values are reported for at least three independent experiments.

***β*-Arrestin Recruitment Assay:** *β*-arrestin 2 recruitment to D_3R was assayed using the DiscoverX Pathhunter kit according to the manufacturer's instructions, with some minor modifications. In brief, CHO-K1 cells expressing human *β*-arrestin 2 tagged with a *β*-galactosidase enzyme lacking part of the catalytic domain, and human D_3R C-terminally tagged with a complementary fragment of *β*-galactosidase, were grown in culture medium (DiscoverX) supplemented with G418 and hygromycin. Cells were seeded into white plastic 96-well plates at a density of 2×10^4 cells/well, 24 h prior to the assay, in a volume of 50 µl/well of Cell Plating Reagent 2 (CP2; DiscoverX).

Test compounds were dissolved in DMSO and diluted to the appropriate concentrations in CP2, added the cells in a volume of 30 µl/well, and pre-incubated with the cells at 37 C for 30 min. Next, dopamine (dissolved and diluted in 30 µl CP2 so as to obtain the various concentrations used to construct concentration-response curves) was applied, followed by another 90 min of incubation at 37 C.

Finally, to detect functional complementation of *β*-galactosidase upon dopamine-induced *β*-arrestin 2 recruitment to D_3R, cells were treated with a detection cocktail containing a coelenterazine-based *β*-galactosidase substrate (as described by the manufacturer), and incubated for another 60 min at room temperature, prior to assay read-out using a Perkin-Elmer Enspire plate reader (luminescence mode; read time 1 s/well).

Molecular Docking Studies: *In silico* molecular docking studies were performed following by the previous study.[52] Compounds **1, 17, 19, 31,** and **32** were drawn on ChemDraw Profession 15.1 (PerkinElmer Informatics, Inc.), then imported to Chem3D Ultra 15.1 (PerkinElmer Informatics, Inc.) to minimize individual structures by MMFF94 force field for preparation of molecular docking. Molecular docking studies were performed via AutoDock 4.2[53] plugin on PyMOL (pymol.org). X-ray structure of dopamine 3 receptor (D_3R) (PDB ID 3PBL, Resolution 2.89 Å) was obtained from RCSB Protein Data Bank (www.rcsb.org). Waters and other heteroatoms were removed from the structure, followed by adding polar hydrogens. Non-polar hydrogens were removed from every compound. A grid box with a dimension of 30 × 30 × 28.2 $Å^3$ was applied to the D_3R X-ray structure, covering orthosteric and secondary binding sites. The Lamarckian Genetic Algorithm with a maximum of 2,500,000 energy evaluations was used to calculate 100 protein-ligand binding poses for each compound to each protein. The protein−ligand complex reported for each compound exhibited the most ligand-protein contacts with the lowest free binding energy.

Data Analysis: Statistical analysis from pharmacological assays were conducted on GraphPad Prism 7.04 software.

ASSOCIATED CONTENT

Supporting Information. The Supporting Information is available free of charge on the ACS Publications website

^1H and ^{13}C NMR spectra and mass spectral data of isolated compounds **E**, **F**, **4a**, **5a-c**, **6a**, **6c-f**, **6h**, **7-24**, **26**, **28-30**, **32**, **34-37**, and LCMS traces of **1** and **31** (PDF)

Molecular formula strings and some data (CSV)

AUTHOR INFORMATION

Corresponding Author

*Phone: (215) 746-8233. E-mail: rmach@pennmedicine.upenn.edu.

ORCID

Sean W. Reilly: 0000-0002-1656-1895

Chia-Ju Hsieh: 0000-0002-2833-7727

Robert H. Mach: 0000-0002-7645-2869

John Karanicolas: 0000-0003-0300-726X

Author Contributions

The manuscript was written through contributions of all authors. All authors have given approval to the final version of the manuscript.

Funding Sources

National Institute on Drug Abuse (Grant R01 DA29840-07 to R.H.M., Grant R01 DA23957-06 to R.R.L.) is gratefully acknowledged for financial support. S.W.R. and A.A.R. are supported by Training Grant 5T32DA028874-08.

ACKNOWLEDGMENTS

K_i determinations, receptor binding profiles, and agonist/antagonist functional data was generously provided by the National Institute of Mental Health's Psychoactive Drug Screening Program, Contract # HHSN-271-2013-00017-C (NIMH PDSP). The NIMH PDSP is Directed by Bryan L. Roth at the University of North Carolina at Chapel Hill and Project Officer Jamie Driscoll at NIMH, Bethesda MD, USA. For experimental details please refer to the PDSP web site https://pdsp.unc.edu/ims/investigator/web/.

ABBREVIATIONS

ACN, acetonitrile; AMP, adenosine monophosphate; CNS, central nervous system; DA, dopamine; DCM, dichloromethane; D_2R, dopamine D_2 receptor; D_3R, dopamine D_3 receptor; GPCR, G-protein coupled receptor; HEK, human embryonic kidney 293; [^{125}I]IABN, [^{125}I]-*N*-benzyl-5-iodo-2,3-dimethoxy[3.3.1]azabicyclononan-3-*β*-ylbenzamide; Pd, palladium; PET, positron emission tomography; TFA, trifluoroacetic acid

REFERENCES

1. Leggio, G. M.; Bucolo, C.; Platania, C. B. M.; Salomone, S.; Drago, F. Current Drug Treatments Targeting Dopamine D3 Receptor. *Pharmacol. Ther.* **2016,** *165*, 164-177.

2. Keck, T. M.; John, W. S.; Czoty, P. W.; Nader, M. A.; Newman, A. H. Identifying Medication Targets for Psychostimulant Addiction: Unraveling the Dopamine D3 Receptor Hypothesis. *J. Med. Chem.* **2015,** *58*, 5361-5380.

3. Strange, P. G. Antipsychotic Drug Action: Antagonism, Inverse Agonism or Partial Agonism. *Trends Pharmacol. Sci.* **2008,** *29*, 314-321.

4. Murray, A. M.; Ryoo, H. L.; Gurevich, E.; Joyce, J. N. Localization of Dopamine D3 Receptors to Mesolimbic and D2 Receptors to Mesostriatal Regions of Human Forebrain. *Proc. Natl. Acad. Sci. U.S.A.* **1994,** *91*, 11271-11275.

5. Heidbreder, C. A.; Newman, A. H. Current Perspectives on Selective Dopamine D3 Receptor Antagonists as Pharmacotherapeutics for Addictions and Related Disorders. *Ann. N. Y. Acad. Sci.* **2010,** *1187*, 4-34.

6. Slifstein, M.; Rabiner, E. A.; Gunn, R. N., Chapter Eleven - Imaging the Dopamine D3 Receptor In Vivo. In *Imaging of the Human Brain in Health and Disease*, Academic Press: Boston, 2014; pp 265-287.

7. Searle, G.; Beaver, J. D.; Comley, R. A.; Bani, M.; Tziortzi, A.; Slifstein, M.; Mugnaini, M.; Griffante, C.; Wilson, A. A.; Merlo-Pich, E.; Houle, S.; Gunn, R.; Rabiner, E. A.; Laruelle, M. Imaging

Dopamine D_3 Receptors in the Human Brain with Positron Emission Tomography, [^{11}C]PHNO, and a Selective D_3 Receptor Antagonist. *Biol. Psychiatry* **2010,** *68*, 392-399.

8. Nebel, N.; Maschauer, S.; Kuwert, T.; Hocke, C.; Prante, O. In Vitro and In Vivo Characterization of Selected Fluorine-18 Labeled Radioligands for PET Imaging of the Dopamine D3 Receptor. *Molecules* **2016,** *21*, 1144.

9. Boileau, I.; Nakajima, S.; Payer, D. Imaging the D3 Dopamine Receptor Across Behavioral and Drug Addictions: Positron Emission Tomography Studies with [11C]-(+)-PHNO. *Eur. Neuropsychopharmacol.* **2015,** *25*, 1410-1420.

10. Wang, Q.; Mach, R. H.; Luedtke, R. R.; Reichert, D. E. Subtype Selectivity of Dopamine Receptor Ligands: Insights from Structure and Ligand-Based Methods. *J. Chem. Inf. Model.* **2010,** *50*, 1970-1985.

11. Newman, A. H.; Beuming, T.; Banala, A. K.; Donthamsetti, P.; Pongetti, K.; LaBounty, A.; Levy, B.; Cao, J.; Michino, M.; Luedtke, R. R.; Javitch, J. A.; Shi, L. Molecular Determinants of Selectivity and Efficacy at the Dopamine D3 Receptor. *J. Med. Chem.* **2012,** *55*, 6689-6699.

12. Chien, E. Y. T.; Liu, W.; Zhao, Q.; Katritch, V.; Won Han, G.; Hanson, M. A.; Shi, L.; Newman, A. H.; Javitch, J. A.; Cherezov, V.; Stevens, R. C. Structure of the Human Dopamine D3 Receptor in Complex with a D2/D3 Selective Antagonist. *Science* **2010,** *330*, 1091-1095.

13. Michino, M.; Beuming, T.; Donthamsetti, P.; Newman, A. H.; Javitch, J. A.; Shi, L. What Can Crystal Structures of Aminergic Receptors Tell Us about Designing Subtype-Selective Ligands? *Pharmacol. Rev.* **2015,** *67*, 198-213.

14. Reilly, S. W.; Griffin, S.; Taylor, M.; Sahlholm, K.; Weng, C.-C.; Xu, K.; Jacome, D. A.; Luedtke, R. R.; Mach, R. H. Highly Selective Dopamine D3 Receptor Antagonists with Arylated Diazaspiro Alkane Cores. *J. Med. Chem.* **2017,** *60*, 9905-9910.

15. Reilly, S. W.; Bryan, N. W.; Mach, R. H. Pd-catalyzed arylation of linear and angular spirodiamine salts under aerobic conditions. *Tetrahedron Lett.* **2017,** *58*, 466-469.

16. Reilly, S. W.; Mach, R. H. Pd-Catalyzed Synthesis of Piperazine Scaffolds Under Aerobic and Solvent-Free Conditions. *Org. Lett.* **2016,** *18*, 5272-5275.

17. Vangveravong, S.; Zhang, Z.; Taylor, M.; Bearden, M.; Xu, J.; Cui, J.; Wang, W.; Luedtke, R. R.; Mach, R. H. Synthesis and Characterization of Selective Dopamine D2 Receptor Ligands Using Aripiprazole as the Lead Compound. *Bioorg. Med. Chem.* **2011,** *19*, 3502-3511.

18. Micheli, F.; Bacchi, A.; Braggio, S.; Castelletti, L.; Cavallini, P.; Cavanni, P.; Cremonesi, S.; Dal Cin, M.; Feriani, A.; Gehanne, S.; Kajbaf, M.; Marchió, L.; Nola, S.; Oliosi, B.; Pellacani, A.; Perdonà, E.; Sava, A.; Semeraro, T.; Tarsi, L.; Tomelleri, S.; Wong, A.; Visentini, F.; Zonzini, L.; Heidbreder, C. 1,2,4-Triazolyl 5-Azaspiro[2.4]heptanes: Lead Identification and Early Lead Optimization of a New Series of Potent and Selective Dopamine D3 Receptor Antagonists. *J. Med. Chem.* **2016,** *59*, 8549-8576.

19. Micheli, F.; Arista, L.; Bertani, B.; Braggio, S.; Capelli, A. M.; Cremonesi, S.; Di-Fabio, R.; Gelardi, G.; Gentile, G.; Marchioro, C.; Pasquarello, A.; Provera, S.; Tedesco, G.; Tarsi, L.; Terreni, S.; Worby, A.; Heidbreder, C. Exploration of the Amine Terminus in a Novel Series of 1,2,4-Triazolo-3-yl-azabicyclo[3.1.0]hexanes as Selective Dopamine D3 Receptor Antagonists. *J. Med. Chem.* **2010,** *53*, 7129-7139.

20. Cremonesi, S.; Micheli, F.; Semeraro, T.; Tarsi, L. Azaspirocyclic Compounds as Dopamine D3 Receptor Antagonists and their Preparation. WO2016067043A1, 2016.

21. Tu, Z.; Li, S.; Cui, J.; Xu, J.; Taylor, M.; Ho, D.; Luedtke, R. R.; Mach, R. H. Synthesis and Pharmacological Evaluation of Fluorine-Containing D3 Dopamine Receptor Ligands. *J. Med. Chem.* **2011,** *54*, 1555-1564.

22. Chu, W.; Tu, Z.; McElveen, E.; Xu, J.; Taylor, M.; Luedtke, R. R.; Mach, R. H. Synthesis and In Vitro Binding of *N*-Phenyl Piperazine Analogs as Potential Dopamine D3 Receptor Ligands. *Bioorg. Med. Chem.* **2005,** *13*, 77-87.

23. Mach, R. H.; Tu, Z.; Xu, J.; Li, S.; Jones, L. A.; Taylor, M.; Luedtke, R. R.; Derdeyn, C. P.; Perlmutter, J. S.; Mintun, M. A. Endogenous Dopamine (DA) Competes with the Binding of a Radiolabeled D(3) Receptor Partial Agonist In Vivo: A Positron Emission Tomography Study. *Synapse* **2011,** *65*, 724-732.

24. Ferreira de Freitas, R.; Schapira, M. A Systematic Analysis of Atomic Protein–Ligand Interactions in the PDB. *MedChemComm* **2017,** *8*, 1970-1981.

25. Wang, S.; Meades, C.; Wood, G.; Osnowski, A.; Anderson, S.; Yuill, R.; Thomas, M.; Mezna, M.; Jackson, W.; Midgley, C.; Griffiths, G.; Fleming, I.; Green, S.; McNae, I.; Wu, S.-Y.; McInnes, C.; Zheleva, D.; Walkinshaw, M. D.; Fischer, P. M. 2-Anilino-4-(thiazol-5-yl)pyrimidine CDK Inhibitors: Synthesis, SAR Analysis, X-ray Crystallography, and Biological Activity. *J. Med. Chem.* **2004,** *47*, 1662-1675.

26. Ananthan, S.; Saini, S. K.; Zhou, G.; Hobrath, J. V.; Padmalayam, I.; Zhai, L.; Bostwick, J. R.; Antonio, T.; Reith, M. E. A.; McDowell, S.; Cho, E.; McAleer, L.; Taylor, M.; Luedtke, R. R. Design, Synthesis, and Structure–Activity Relationship Studies of a Series of [4-(4-Carboxamidobutyl)]-1-arylpiperazines: Insights into Structural Features Contributing to Dopamine D3 versus D2 Receptor Subtype Selectivity. *J. Med. Chem.* **2014,** *57*, 7042-7060.

27. Michino, M.; Donthamsetti, P.; Beuming, T.; Banala, A.; Duan, L.; Roux, T.; Han, Y.; Trinquet, E.; Newman, A. H.; Javitch, J. A.; Shi, L. A Single Glycine in Extracellular Loop 1 Is the Critical Determinant for Pharmacological Specificity of Dopamine D2 and D3 Receptors. *Mol. Pharmacol.* **2013,** *84*, 854-864.

28. Lane, J. R.; Donthamsetti, P.; Shonberg, J.; Draper-Joyce, C. J.; Dentry, S.; Michino, M.; Shi, L.; López, L.; Scammells, P. J.; Capuano, B.; Sexton, P. M.; Javitch, J. A.; Christopoulos, A. A New Mechanism of Allostery in a G Protein–Coupled Receptor Dimer. *Nat. Chem. Biol.* **2014,** *10*, 745-752.

29. Silvano, E.; Millan, M. J.; la Cour, C. M.; Han, Y.; Duan, L.; Griffin, S. A.; Luedtke, R. R.; Aloisi, G.; Rossi, M.; Zazzeroni, F.; Javitch, J. A.; Maggio, R. The Tetrahydroisoquinoline Derivative SB269,652 Is an Allosteric Antagonist at Dopamine D3 and D2 Receptors. *Mol. Pharmacol.* **2010,** *78*, 925-934.

30. Christopoulos, A.; Kenakin, T. G Protein-Coupled Receptor Allosterism and Complexing. *Pharmacol. Rev.* **2002,** *54*, 323-374.

31. Gerald, P.; Friedrich, B.; Elisabeth, K. Construction of Antagonist Dose-Response Curves for Estimation of pA2-Values by Schild-Plot Analysis and Detection of Allosteric Interactions. *Br. J. Pharmacol.* **1992,** *106*, 710-716.

32. Kumar, V.; Moritz, A. E.; Keck, T. M.; Bonifazi, A.; Ellenberger, M. P.; Sibley, C. D.; Free, R. B.; Shi, L.; Lane, J. R.; Sibley, D. R.; Newman, A. H. Synthesis and Pharmacological Characterization of Novel trans-Cyclopropylmethyl-Linked Bivalent Ligands That Exhibit Selectivity and Allosteric Pharmacology at the Dopamine D3 Receptor (D3R). *J. Med. Chem.* **2017,** *60*, 1478-1494.

33. Shonberg, J.; Draper-Joyce, C.; Mistry, S. N.; Christopoulos, A.; Scammells, P. J.; Lane, J. R.; Capuano, B. Structure–Activity Study of N-((trans)-4-(2-(7-Cyano-3,4-dihydroisoquinolin-2(1H)-yl)ethyl)cyclohexyl)-1H-indole-2-carboxamide (SB269652), a Bitopic Ligand That Acts as a Negative Allosteric Modulator of the Dopamine D2 Receptor. *J. Med. Chem.* **2015,** *58*, 5287-5307.

34. Mistry, S. N.; Shonberg, J.; Draper-Joyce, C. J.; Klein Herenbrink, C.; Michino, M.; Shi, L.; Christopoulos, A.; Capuano, B.; Scammells, P. J.; Lane, J. R. Discovery of a Novel Class of Negative Allosteric Modulator of the Dopamine D2 Receptor Through Fragmentation of a Bitopic Ligand. *J. Med. Chem.* **2015,** *58*, 6819-6843.

35. Kroeze, W. K.; Sassano, M. F.; Huang, X.-P.; Lansu, K.; McCorvy, J. D.; Giguère, P. M.; Sciaky, N.; Roth, B. L. PRESTO-Tango as an Open-Source Resource for Interrogation of the Druggable Human GPCRome. *Nat. Struct. Mol. Biol* **2015,** *22*, 362.

36. Besnard, J.; Ruda, G. F.; Setola, V.; Abecassis, K.; Rodriguiz, R. M.; Huang, X.-P.; Norval, S.; Sassano, M. F.; Shin, A. I.; Webster, L. A.; Simeons, F. R. C.; Stojanovski, L.; Prat, A.; Seidah, N. G.; Constam, D. B.; Bickerton, G. R.; Read, K. D.; Wetsel, W. C.; Gilbert, I. H.; Roth, B. L.; Hopkins, A. L. Automated Design of Ligands to Polypharmacological Profiles. *Nature* **2012,** *492*, 215.

37. Luedtke, R. R.; Freeman, R. A.; Boundy, V. A.; Martin, M. W.; Huang, Y.; Mach, R. H. Characterization of 125I-IABN, A Novel Azabicyclononane Benzamide Selective for D2-Like Dopamine Receptors. *Synapse* **2000,** *38*, 438-449.

38. Baker, J. G.; Hill, S. J. Multiple GPCR conformations and signalling pathways: implications for antagonist affinity estimates. *Trends Pharmacol. Sci.* **2007,** *28*, 374-381.

39. Boateng, C. A.; Bakare, O. M.; Zhan, J.; Banala, A. K.; Burzynski, C.; Pommier, E.; Keck, T. M.; Donthamsetti, P.; Javitch, J. A.; Rais, R.; Slusher, B. S.; Xi, Z.-X.; Newman, A. H. High Affinity Dopamine D3 Receptor (D3R)-Selective Antagonists Attenuate Heroin Self-Administration in Wild-Type but not D3R Knockout Mice. *J. Med. Chem.* **2015,** *58*, 6195-6213.

40. Mach, R. H. Small Molecule Receptor Ligands for PET Studies of the Central Nervous System—Focus on G Protein Coupled Receptors. *Semin. Nucl. Med.* **2017,** *47*, 524-535.

41. Mach, R. H.; Luedtke, R. R. Challenges in the Development of Dopamine D2- and D3-Selective Radiotracers for PET Imaging Studies. *J. Label. Compd. Radiopharm.* **2018,** *61*, 291-298.

42. Sóvágó, J.; Farde, L.; Halldin, C.; Langer, O.; Laszlovszky, I.; Kiss, B.; Gulyás, B. Positron Emission Tomographic Evaluation of the Putative Dopamine-D3 Receptor Ligand, [11C]RGH-1756 in the Monkey Brain. *Neurochem. Int.* **2004,** *45*, 609-617.

43. Kuhnast, B.; Valette, H.; Besret, L.; Demphel, S.; Coulon, C.; Ottaviani, M.; Guillermier, M.; Bottlaender, M.; Dollé, F. Synthesis and Radiolabeling of N-[4-[4-(2-[11C]Methoxyphenyl)piperazin-1-yl]butyl]benzo[b]thiophene-2-carboxamide — a Potential Radiotracer for D3 Receptor Imaging with PET. *Nucl. Med. Biol.* **2006,** *33*, 785-795.

44. Reid, J. L. Alpha-Adrenergic Receptors and Blood Pressure Control. *Am. J. Cardiol.* **1986,** *57*, E6-E12.

45. Newman, A. H.; Grundt, P.; Nader, M. A. Dopamine D3 Receptor Partial Agonists and Antagonists as Potential Drug Abuse Therapeutic Agents. *J. Med. Chem.* **2005,** *48*, 3663-3679.

46. Pilla, M.; Perachon, S.; Sautel, F.; Garrido, F.; Mann, A.; Wermuth, C. G.; Schwartz, J.-C.; Everitt, B. J.; Sokoloff, P. Selective Inhibition of Cocaine-Seeking Behaviour by a Partial Dopamine D3 Receptor Agonist. *Nature* **1999,** *400*, 371-375.

47. Sánchez-Soto, M.; Casadó-Anguera, V.; Yano, H.; Bender, B. J.; Cai, N.-S.; Moreno, E.; Canela, E. I.; Cortés, A.; Meiler, J.; Casadó, V.; Ferré, S. α2A- and α2C-Adrenoceptors as Potential Targets for Dopamine and Dopamine Receptor Ligands. *Mol. Neurobiol.* **2018,** *55*, 8438-8454.

48. Appel, N. M.; Li, S. H.; Holmes, T. H.; Acri, J. B. Dopamine D3 Receptor Antagonist (GSK598809) Potentiates the Hypertensive Effects of Cocaine in Conscious, Freely-Moving Dogs. *J. Pharmacol. Exp. Ther.* **2015,** *354*, 484-492.

49. Galaj, E.; Ewing, S.; Ranaldi, R. Dopamine D1 and D3 Receptor Polypharmacology as a Potential Treatment Approach for Substance use Disorder. *Neurosci. Biobehav. Rev.* **2018,** *89*, 13-28.

50. Hayatshahi, H. S.; Xu, K.; Griffin, S. A.; Taylor, M.; Mach, R. H.; Liu, J.; Luedtke, R. R. Analogues of Arylamide Phenylpiperazine Ligands To Investigate the Factors Influencing D3 Dopamine Receptor Bitropic Binding and Receptor Subtype Selectivity. *ACS Chem. Neurosci.* **2018,** *9*, 2972-2983.

51. Yung-Chi, C.; Prusoff, W. H. Relationship Between the Inhibition Constant (KI) and the Concentration of Inhibitor Which Causes 50 Percent Inhibition (I50) of an Enzymatic Reaction. *Biochem. Pharmacol.* **1973,** *22*, 3099-3108.

52. Reilly, S. W.; Puentes, L. N.; Wilson, K.; Hsieh, C.-J.; Weng, C.-C.; Makvandi, M.; Mach, R. H. Examination of Diazaspiro Cores as Piperazine Bioisosteres in the Olaparib Framework Shows Reduced DNA Damage and Cytotoxicity. *J. Med. Chem.* **2018,** *61*, 5367-5379.

53. Morris, G. M.; Huey, R.; Lindstrom, W.; Sanner, M. F.; Belew, R. K.; Goodsell, D. S.; Olson, A. J. AutoDock4 and AutoDockTools4: Automated Docking with Selective Receptor Flexibility. *J. Comput. Chem.* **2009,** *30*, 2785-2791.

TOC Graphic

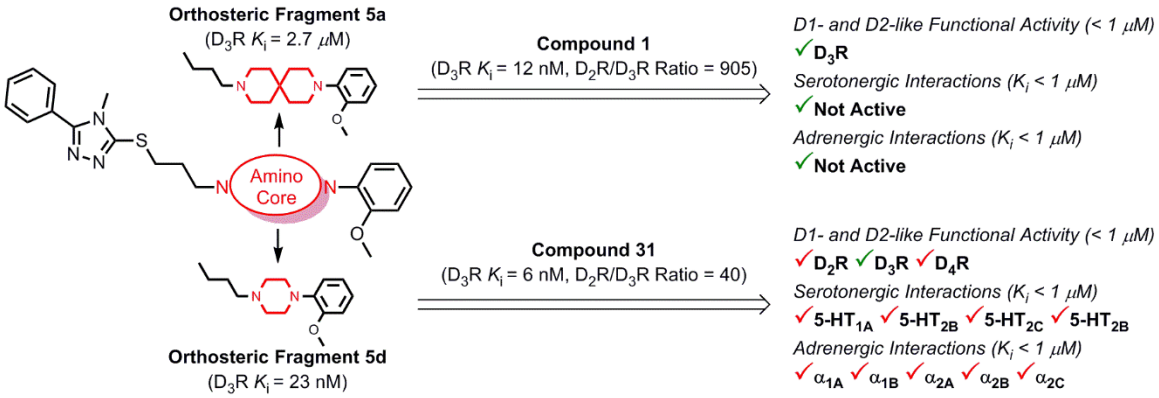
Orthosteric Fragment 5a
(D3R Ki = 2.7 μM)
Amino Core
Orthosteric Fragment 5d
(D3R Ki = 23 nM)
Compound 1
(D3R Ki = 12 nM, D2R/D3R Ratio = 905)
Compound 31
(D3R Ki = 6 nM, D2R/D3R Ratio = 40)
D1- and D2-like Functional Activity (< 1 μM)
✓D3R
Serotonergic Interactions (Ki < 1 μM)
✓Not Active
Adrenergic Interactions (Ki < 1 μM)
✓Not Active
D1- and D2-like Functional Activity (< 1 μM)
✓D2R ✓D3R ✓D4R
Serotonergic Interactions (Ki < 1 μM)
✓5-HT1A ✓5-HT2B ✓5-HT2C ✓5-HT2B
Adrenergic Interactions (Ki < 1 μM)
✓α1A ✓α1B ✓α2A ✓α2B ✓α2C